Electronic supplementary materials *Mendeleev Commun.*, 2024, **34**, 899–901

Nickel nanoparticles formation during Ni catalyst activation revealed by identical location electron microscopy

Anton E. Dzhusupov and Evgeniy O. Pentsak

Table of content

Experimental section

All reagents were purchased and used in their original form: nickel (II) nitrate hexahydrate, tetraethoxysilane (TEOS), 25% aqueous ammonia solution, concentrated hydrochloric acid.

The catalyst was synthesized by heterophase sol-gel method. A typical procedure is described below.

A prepared solution containing distilled water, ethanol and HCl was added in TEOS (40 wt.% silicon oxide) with vigorous stirring. The solution was kept at room temperature for 72 hours. The required portion of nickel (II) nitrate hexahydrate was calculated referred to a metallic nickel. The nickel salt was dissolved in 25% aqueous ammonia solution. The solution was added to distilled water at room temperature at vigorous stirring. Then the flaky precipitate was filtered off and washed with deionized water to remove ammonium nitrate. The resulting precipitate was dried in oven at 110 ℃ and then calcined at 250 ℃ for 4 hours. The obtained powder was mixed with hydralizate prepared earlier. The mixture was adjusted to the consistency of a homogenous paste and dried in the oven at 150 ℃ for 1 hour. After that catalyst precursor is activated in hydrogen flow at a desired temperature.

The resulting catalyst was attached by carbon tape on the surface of an aluminum stub with a diameter of 25 mm for recording images using SEM. The morphology of the samples was studied under native conditions in order to exclude surface effects from sputtering of the conducting layer. The microstructure of the samples was studied by SEM using a Hitachi SU8000 field emission microscope. The images were recorded in the secondary electron detection mode at an accelerating voltage of 10 kV and an operating distance of 8-10 mm.

Also resulting catalyst was studied using TEM. Before measurements the samples were mounted on a 3 mm copper grid with lacey carbon film and fixed in a grid holder. Samples morphology was studied using Hitachi HT7700 transmission electron microscope (TEM). Images were acquired in bright-field TEM mode at 100 kV accelerating voltage.

Then stub with the deposited sample was placed in the reactor and heated in a hydrogen current at 400 ℃ for 4 hours. After reduction, the microparticles deposited on the stub were re-examined using SEM. The phase composition of the catalyst was determined before and after reduction by X-ray diffraction (XRD).

The phase composition of the synthesized materials was determined by X-ray diffractometry (Rigaku Miniflex 600 diffractometer, Japan), a detector with a graphite monochromator and a copper anticathode, an operating voltage of 40 kV, an operating current of 15 mA, Cu-Kα radiation, $\lambda = 1.54187$ Å. The samples were photographed in the range of 2 ° angles from 3 ° to 120 ° in 0.02 ° increments at a shooting speed of 4 °/min.

Figure S1. Samples on microscopy stub in the reactor.

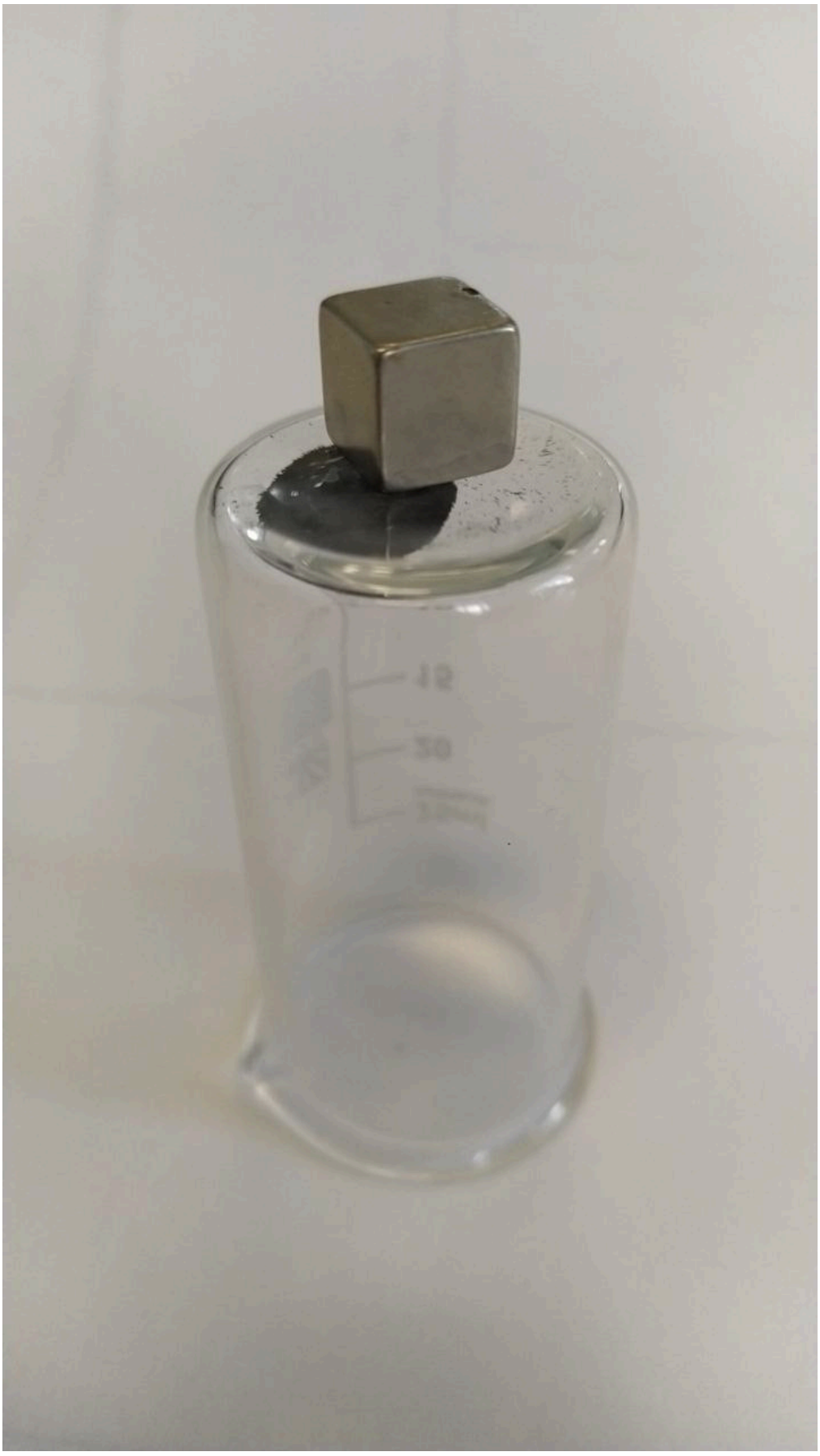

Figure S2. Ferromagnetic properties of activated Ni catalyst.

SEM images of catalyst before reduction

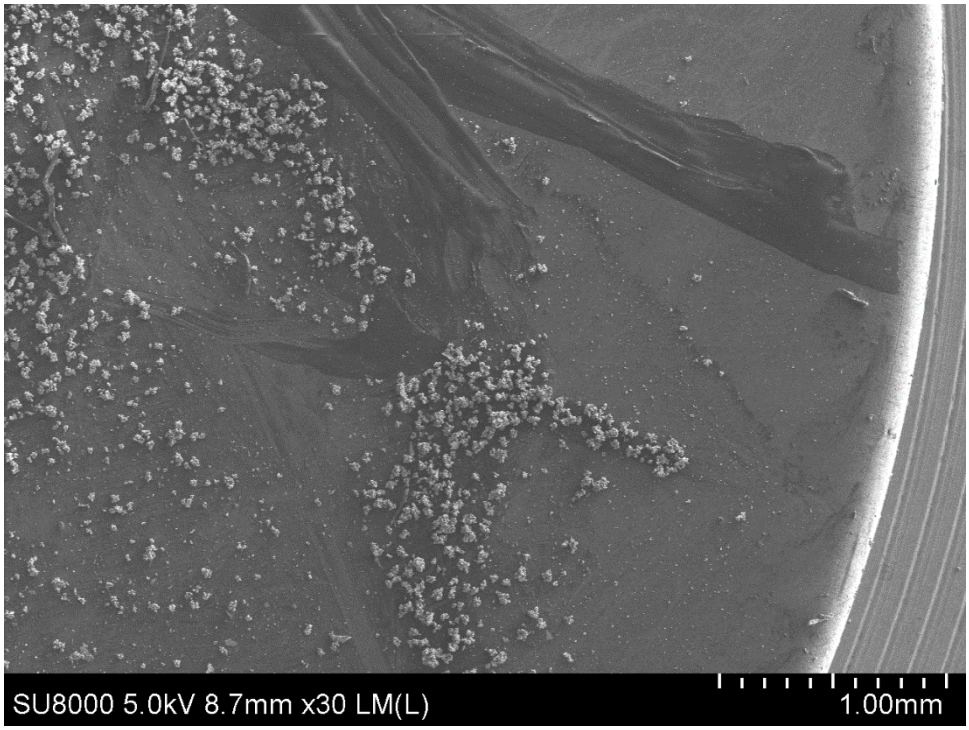

Figure S3. SEM image of catalyst before reduction.

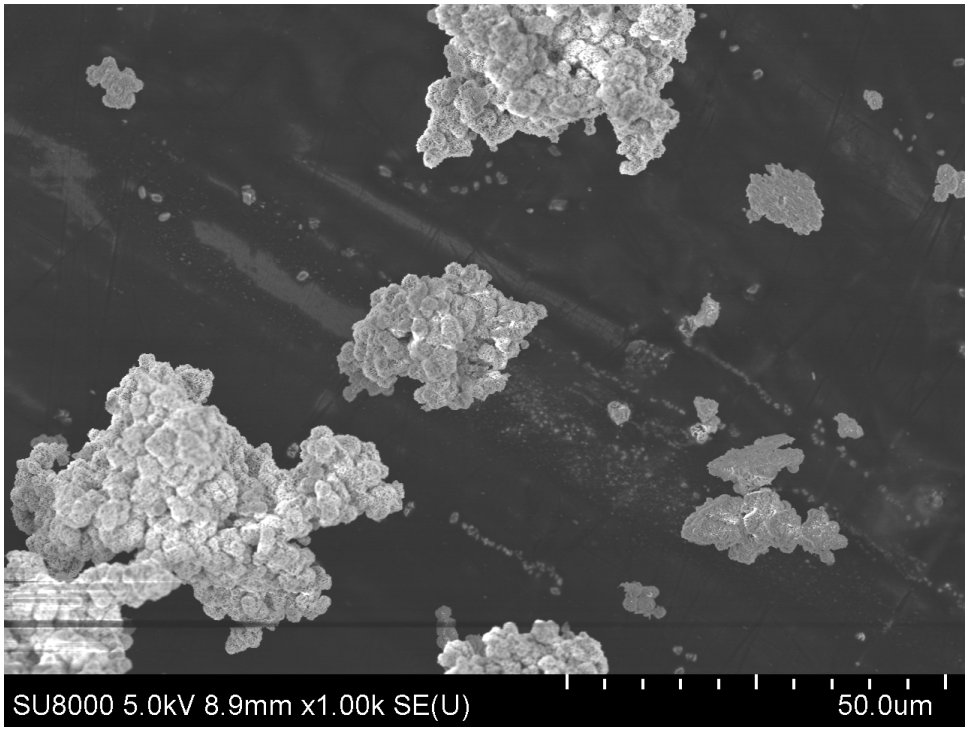

Figure S4. SEM image of catalyst before reduction.

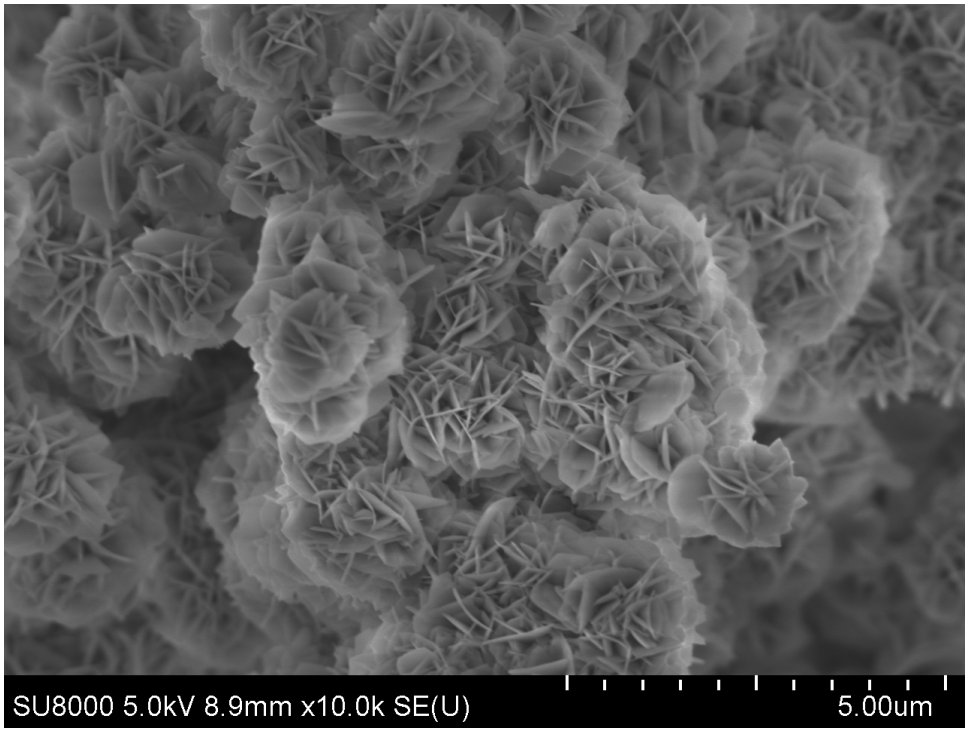

Figure S5. SEM image of catalyst before reduction.

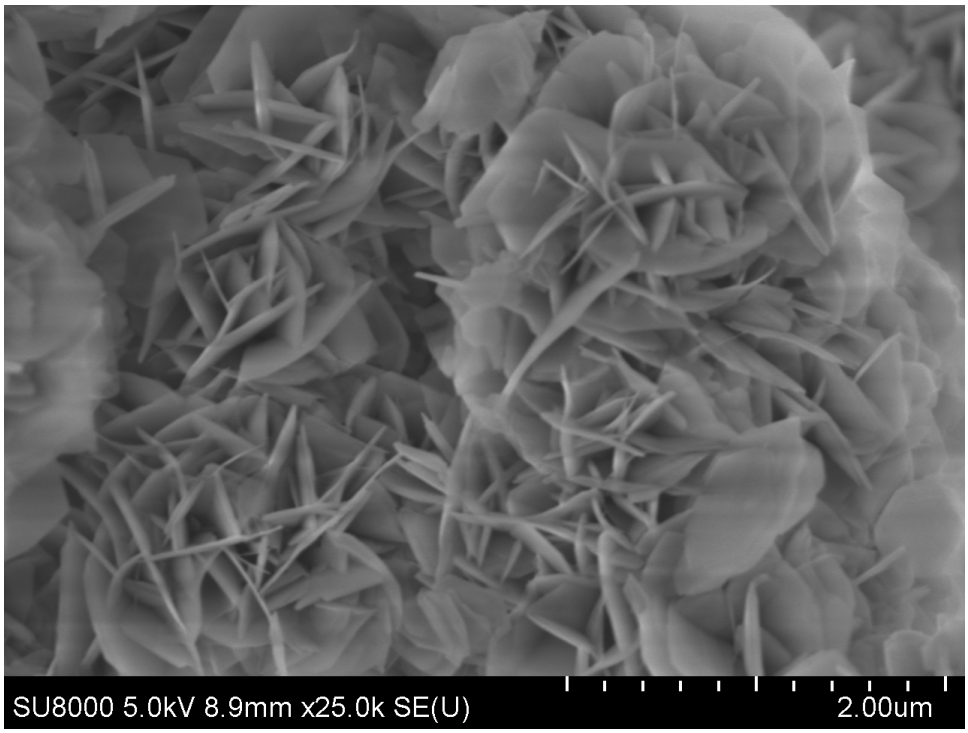

Figure S6. SEM image of catalyst before reduction.

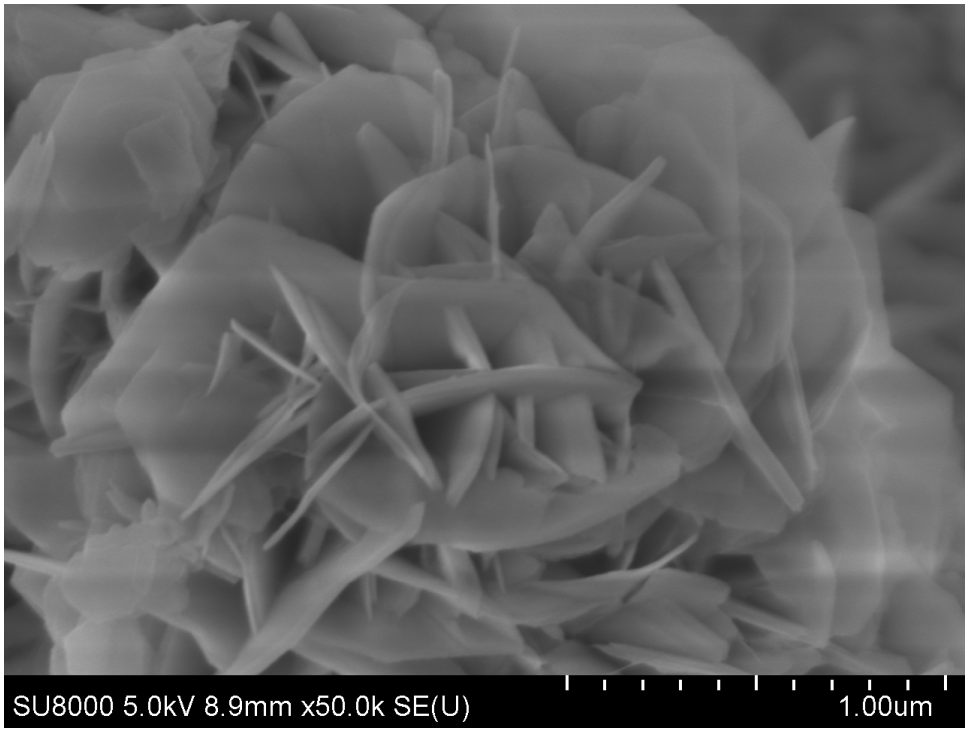

Figure S7. SEM image of catalyst before reduction.

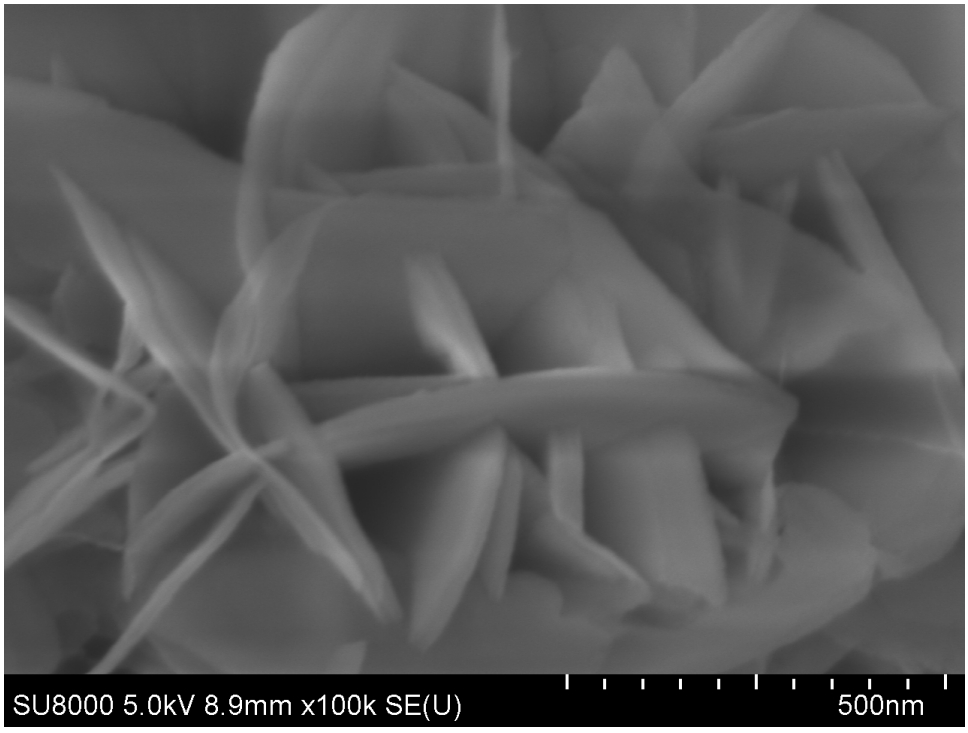

Figure S8. SEM image of catalyst before reduction.

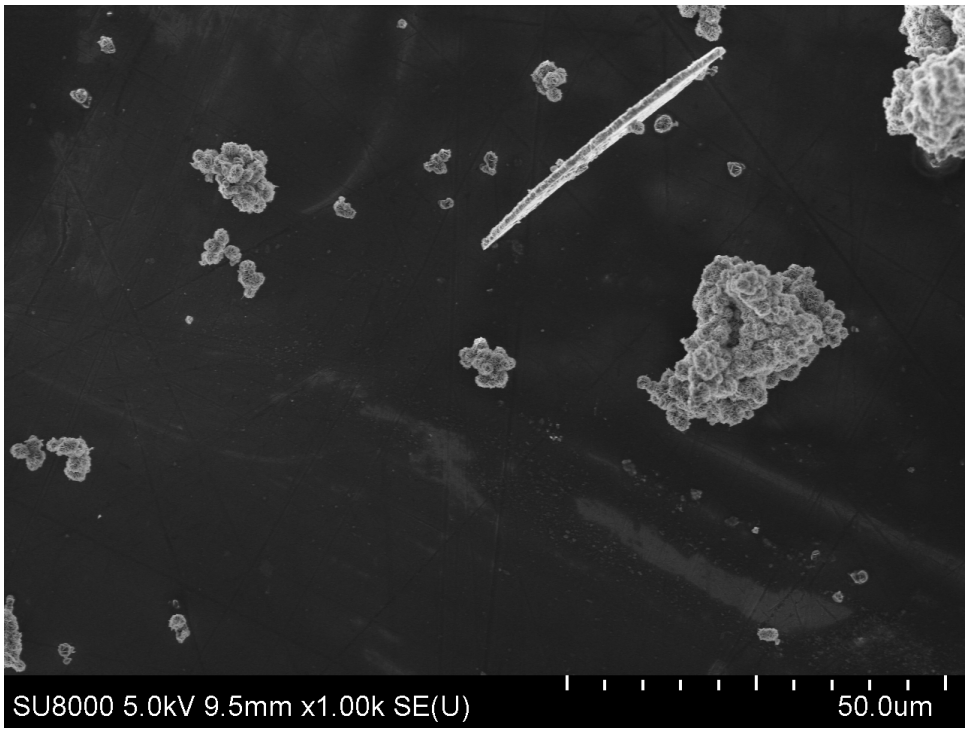

Figure S9. SEM image of catalyst before reduction.

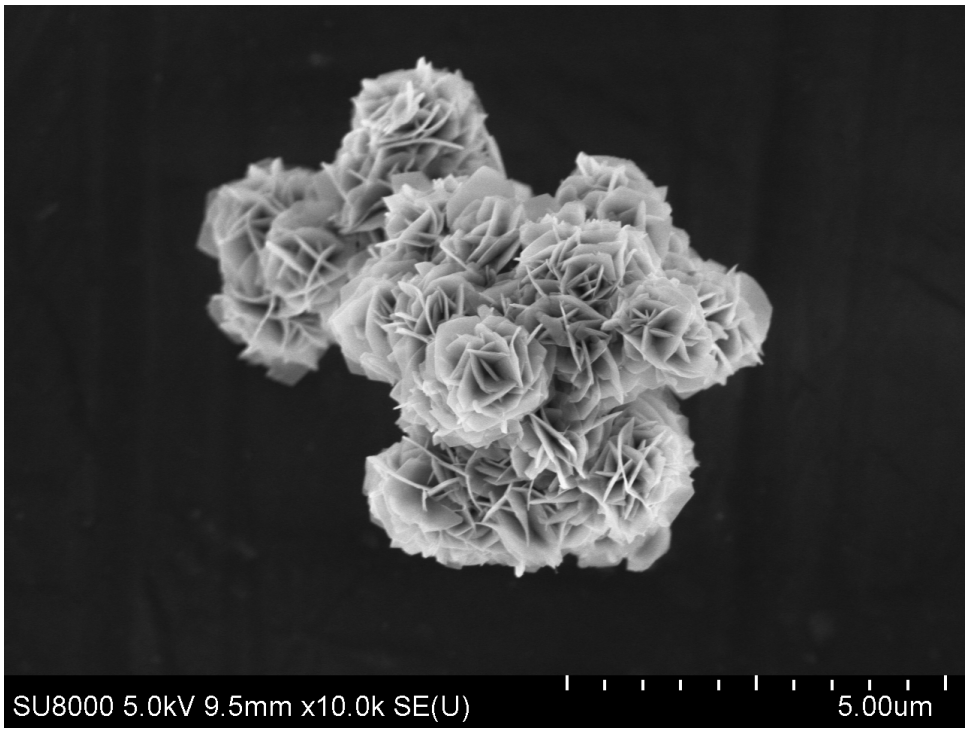

Figure S10. SEM image of catalyst before reduction.

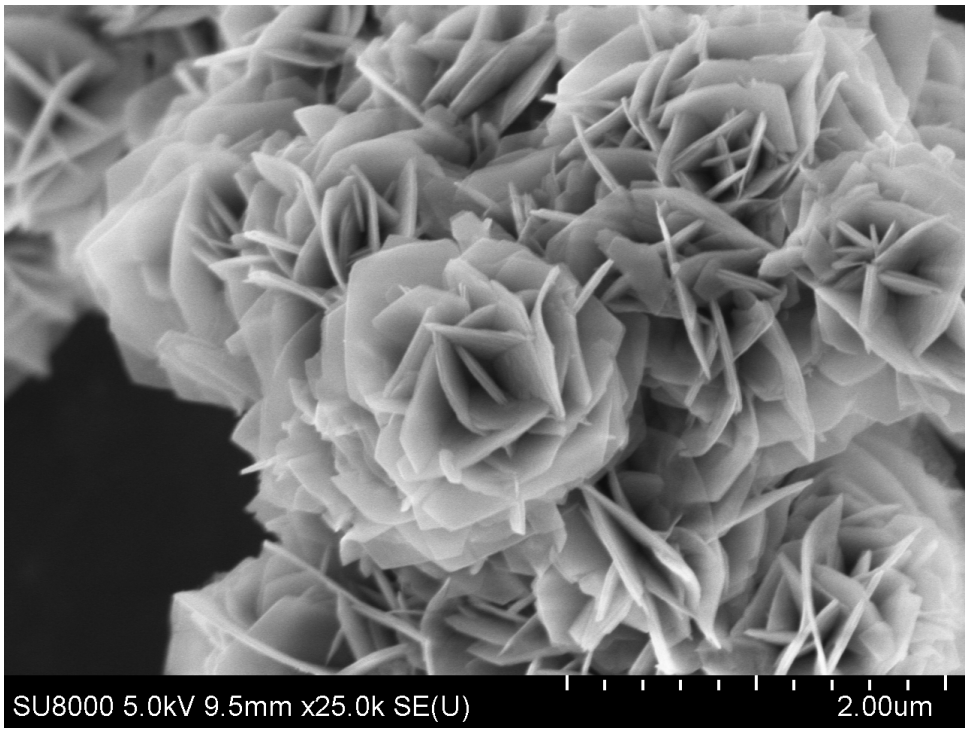

Figure S11. SEM image of catalyst before reduction.

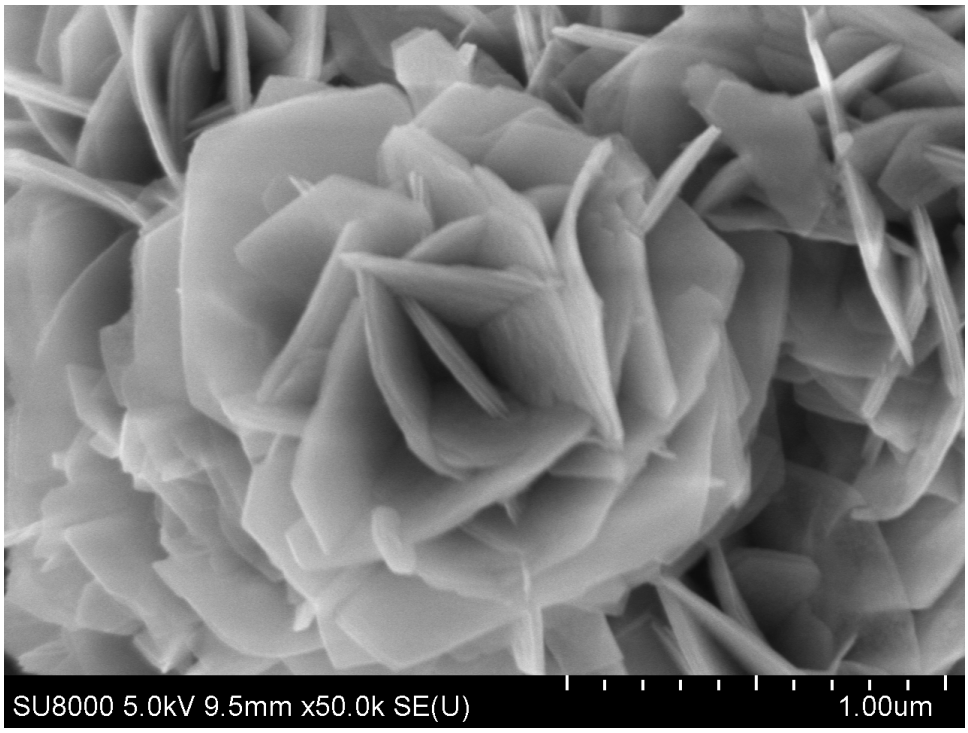

Figure S12. SEM image of catalyst before reduction.

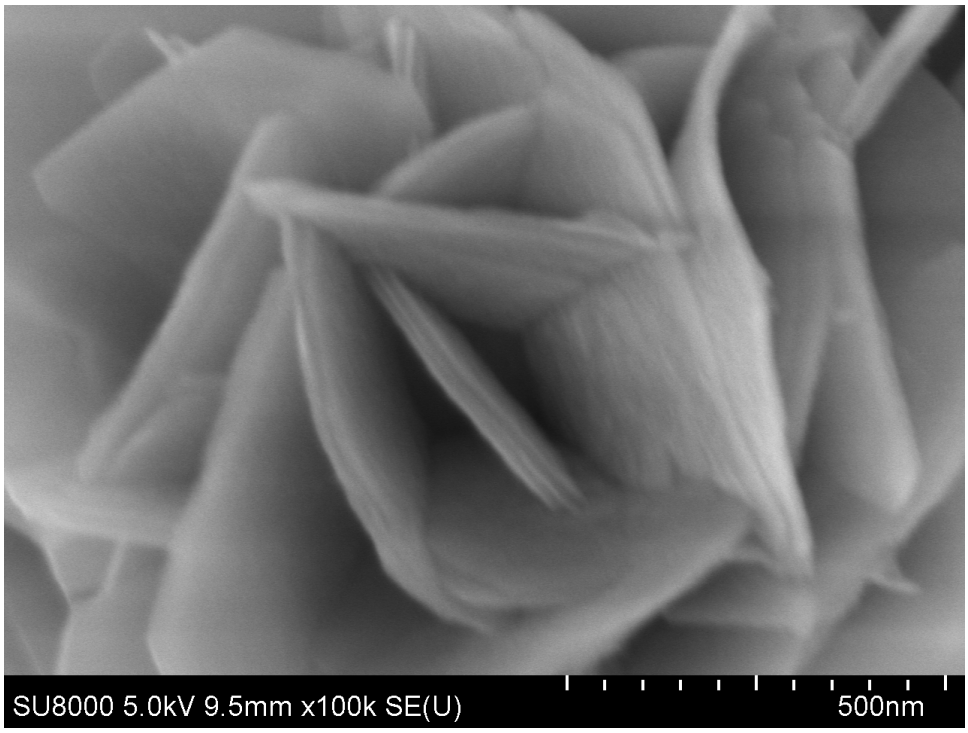

Figure S13. SEM image of catalyst before reduction.

SEM images of catalyst after reduction at 200 ℃

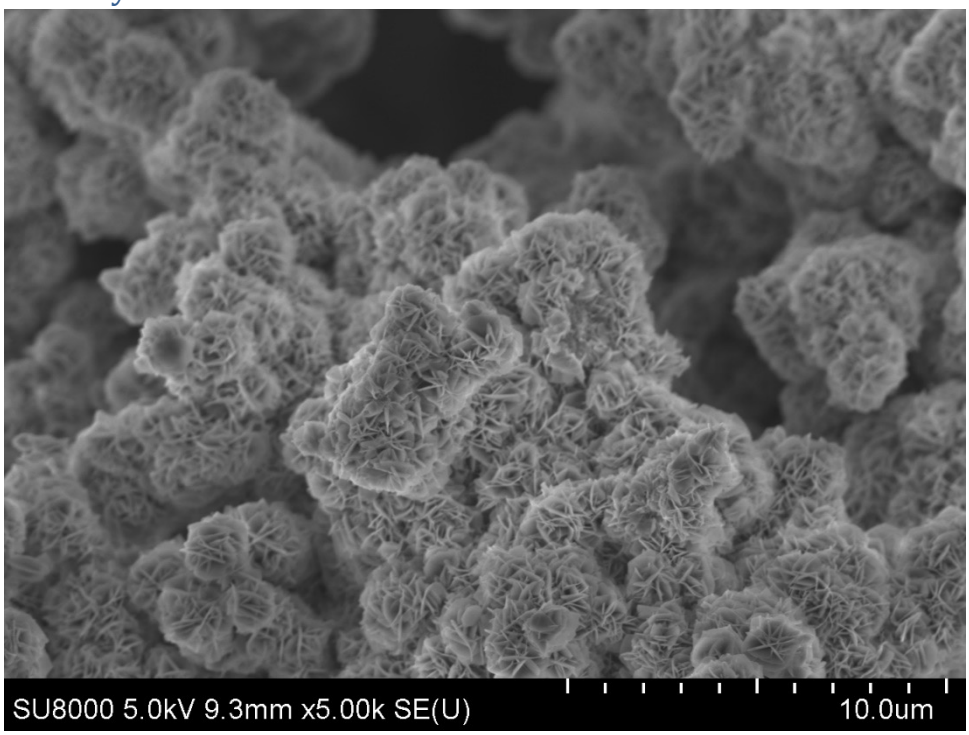

Figure S14. SEM image of catalyst after reduction at 200 ℃.

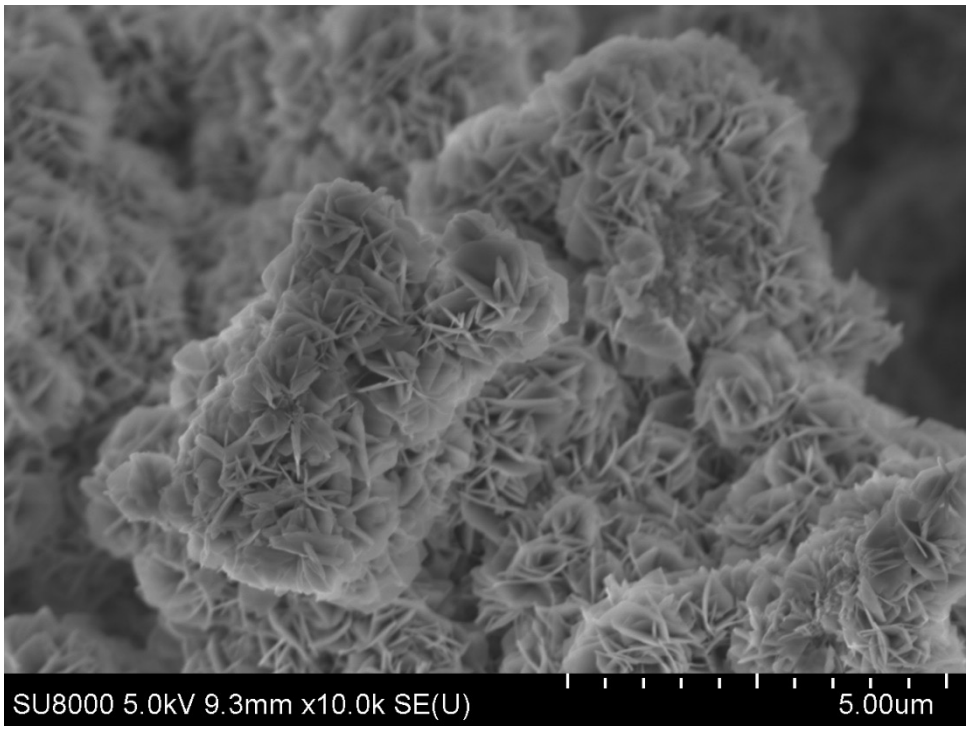

Figure S15. SEM image of catalyst after reduction at 200 ℃.

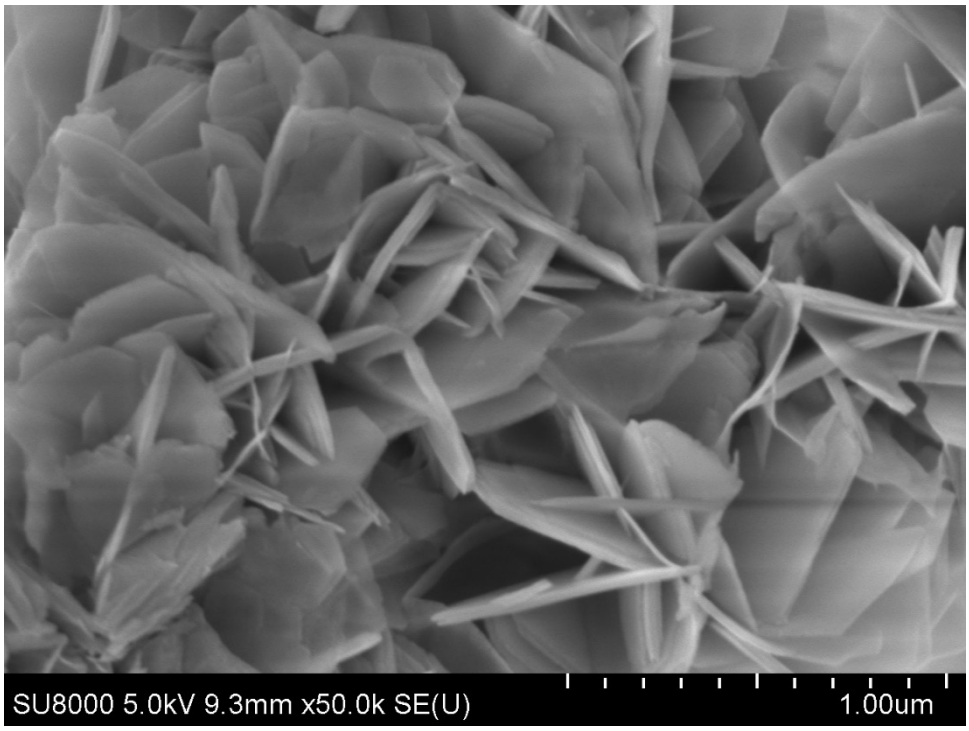

Figure S16. SEM image of catalyst after reduction at 200 ℃.

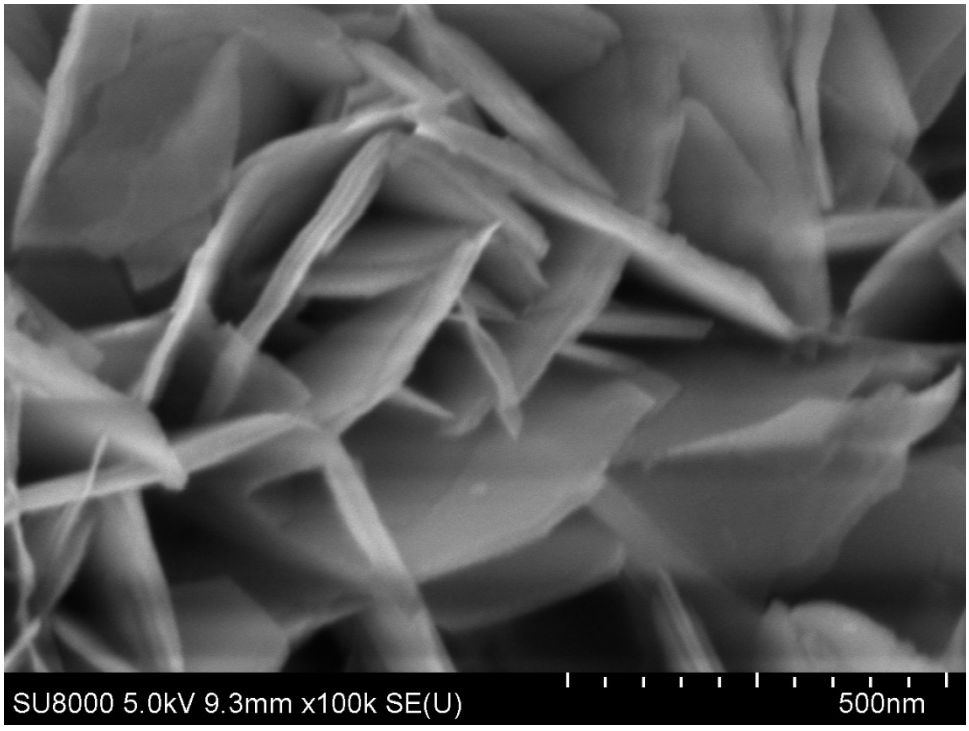

Figure S17. SEM image of catalyst after reduction at 200 ℃.

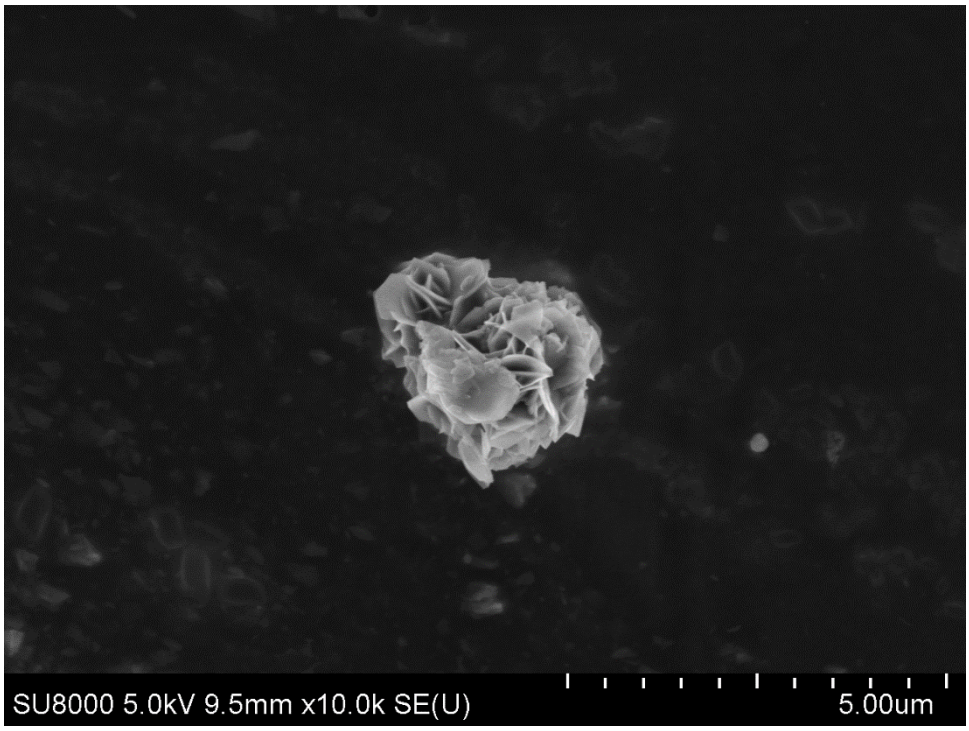

Figure S18. SEM image of catalyst after reduction at 200 ℃.

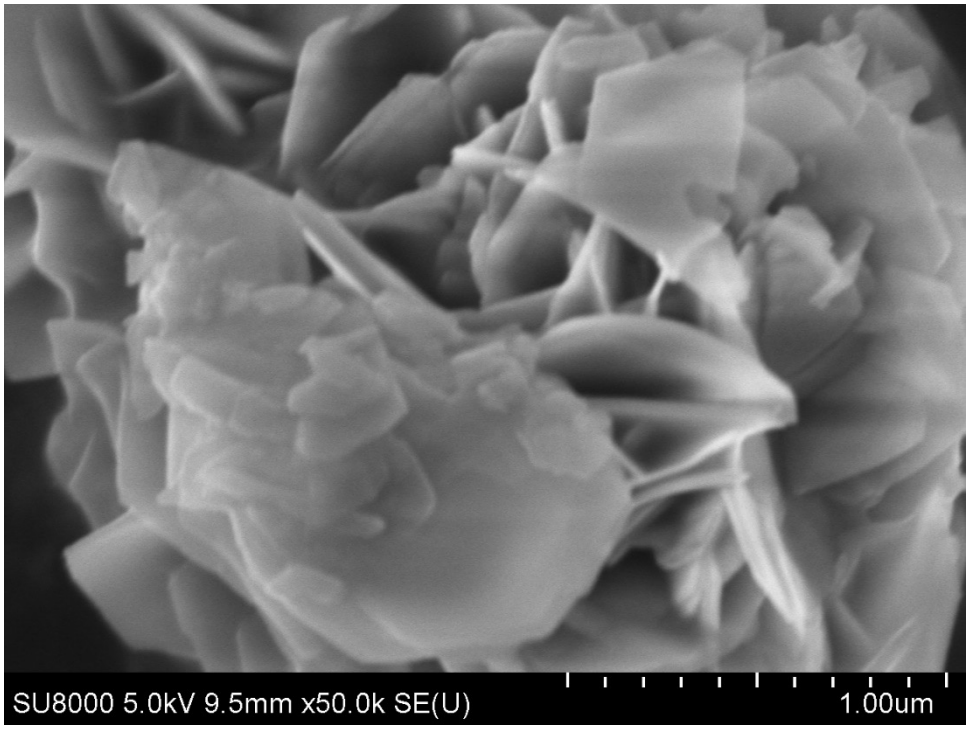

Figure S19. SEM image of catalyst after reduction at 200 ℃.

SEM images of catalyst after reduction at 400 ℃

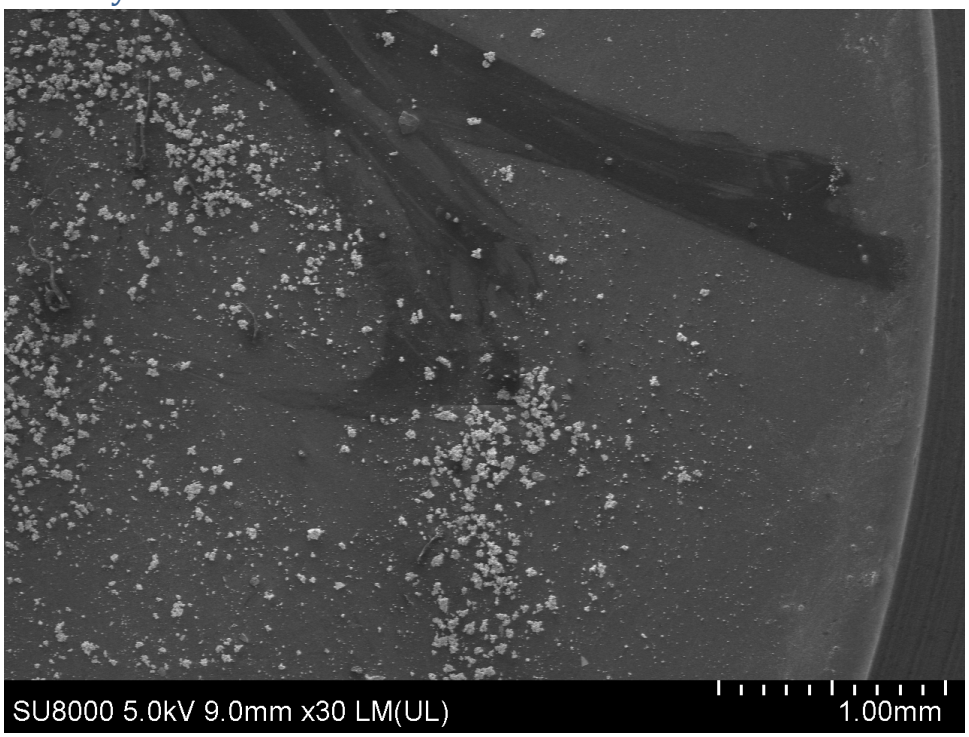

Figure S20. SEM image of catalyst after reduction at 400 ℃.

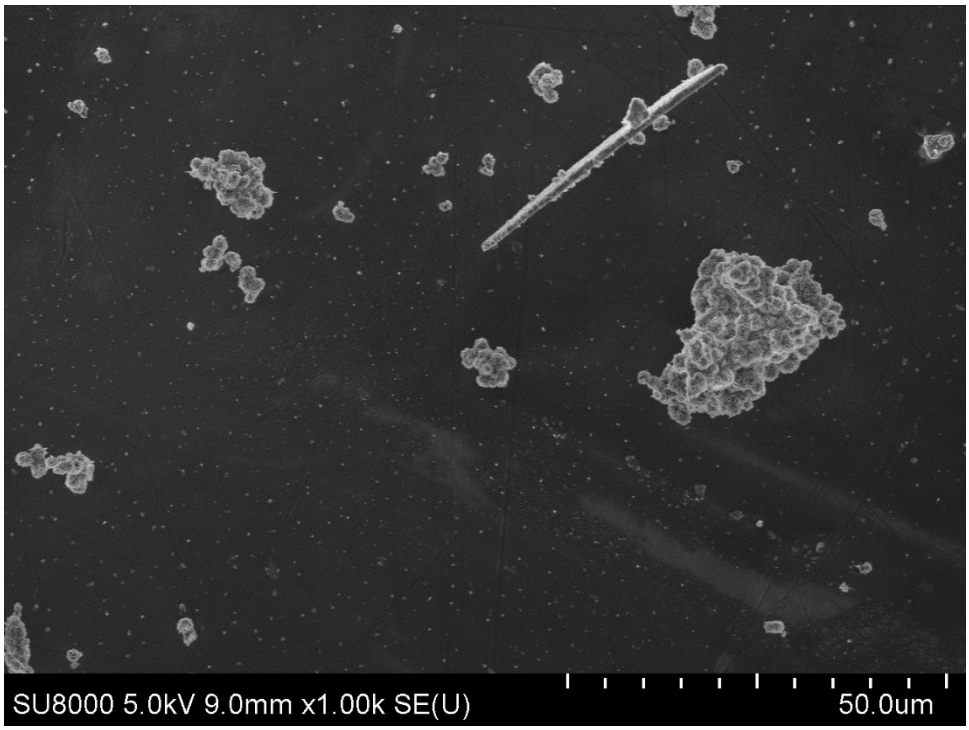

Figure S21. SEM image of catalyst after reduction at 400 ℃.

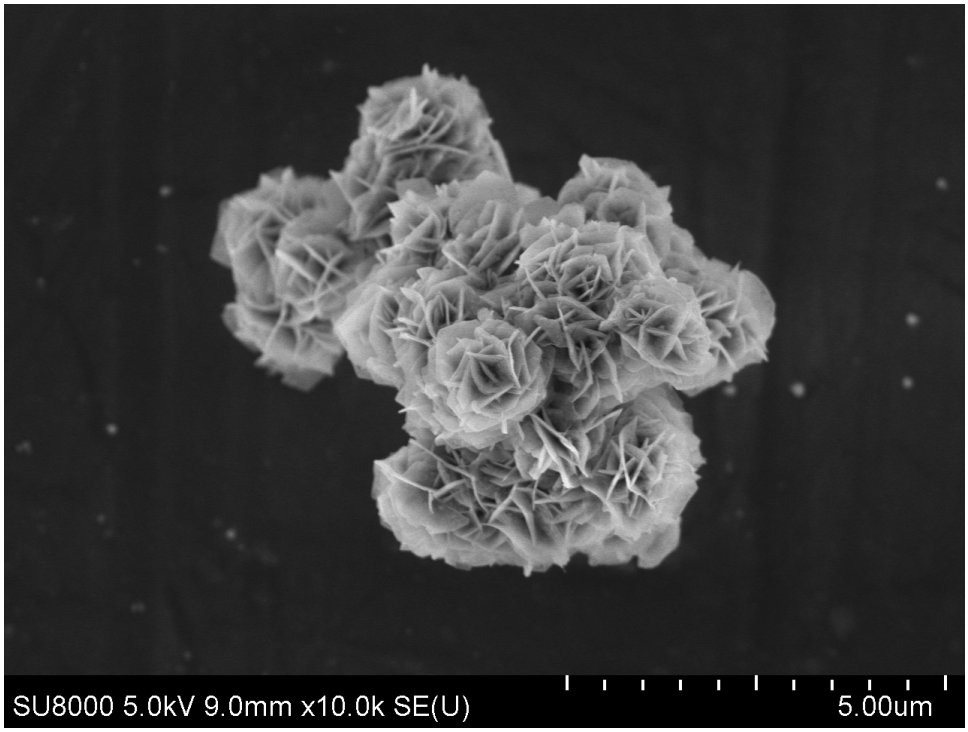

Figure S22. SEM image of catalyst after reduction at 400 ℃.

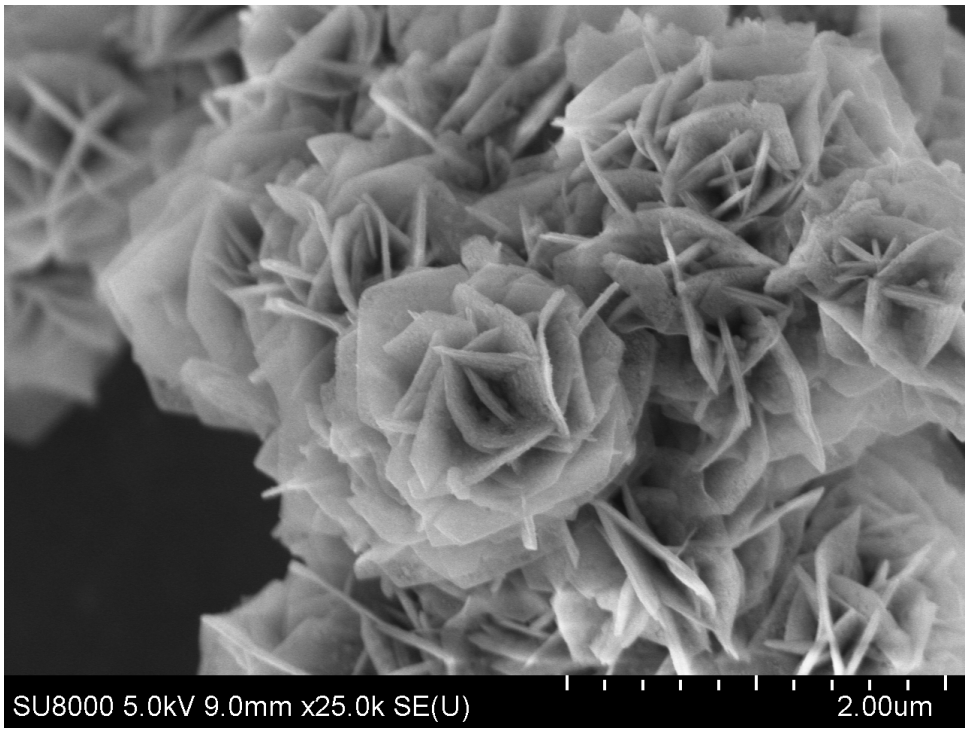

Figure S23. SEM image of catalyst after reduction at 400 ℃.

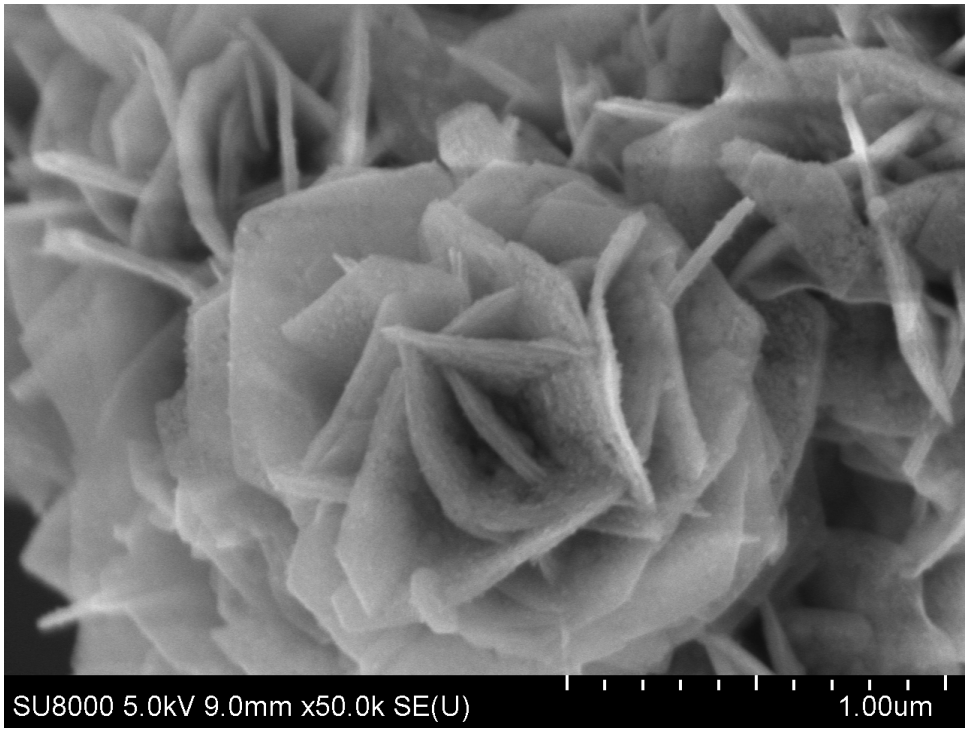

Figure S24. SEM image of catalyst after reduction at 400 ℃.

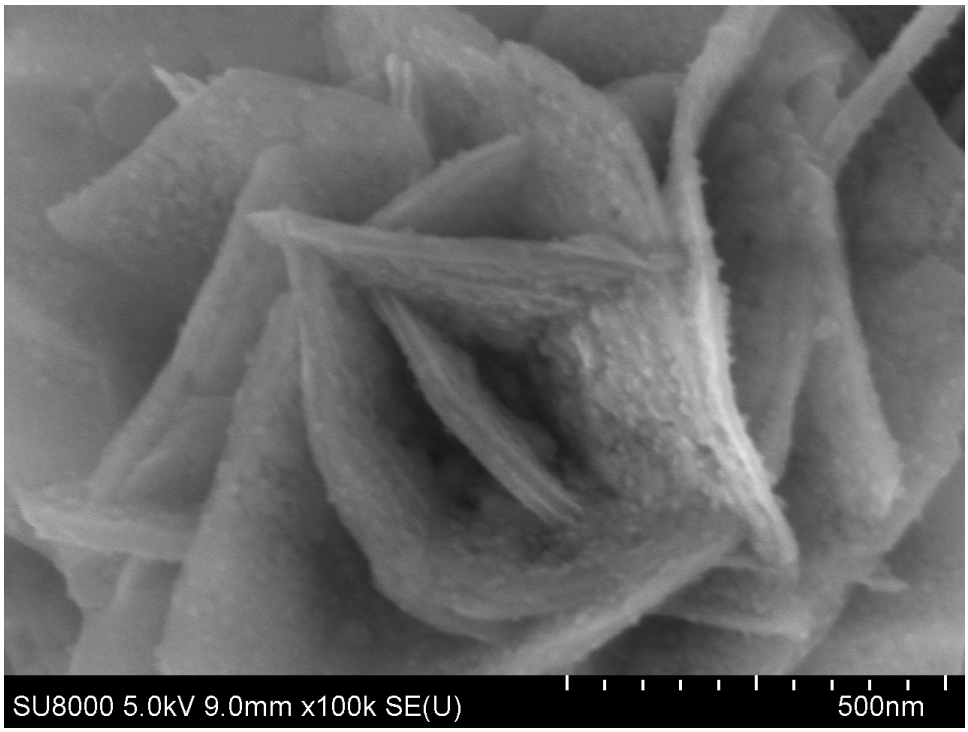

Figure S25. SEM image of catalyst after reduction at 400 ℃.

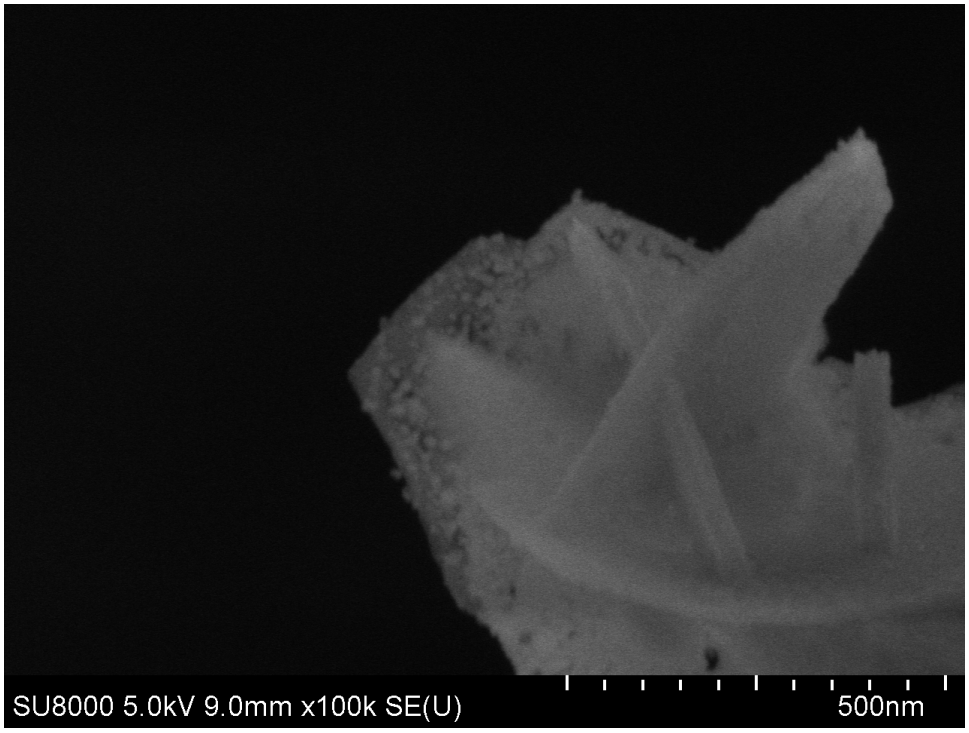

Figure S26. SEM image of catalyst after reduction at 400 °C.

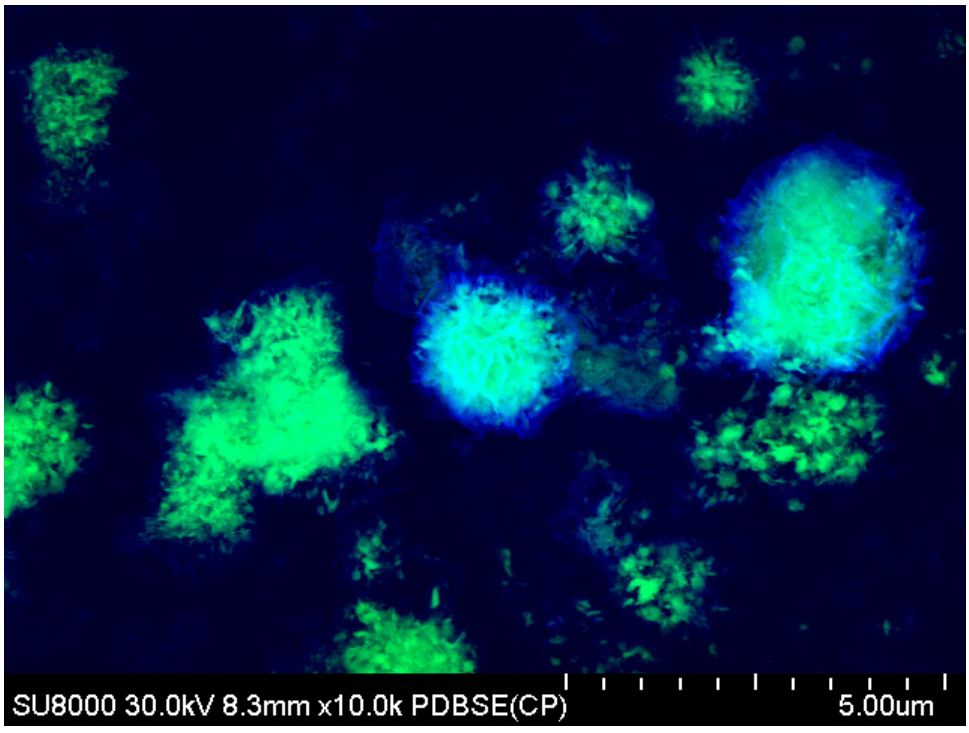

Figure S27. SEM image of catalyst after reduction at 400 °C (blue area – signal from SE detector, green-area – from PDBSE detector).

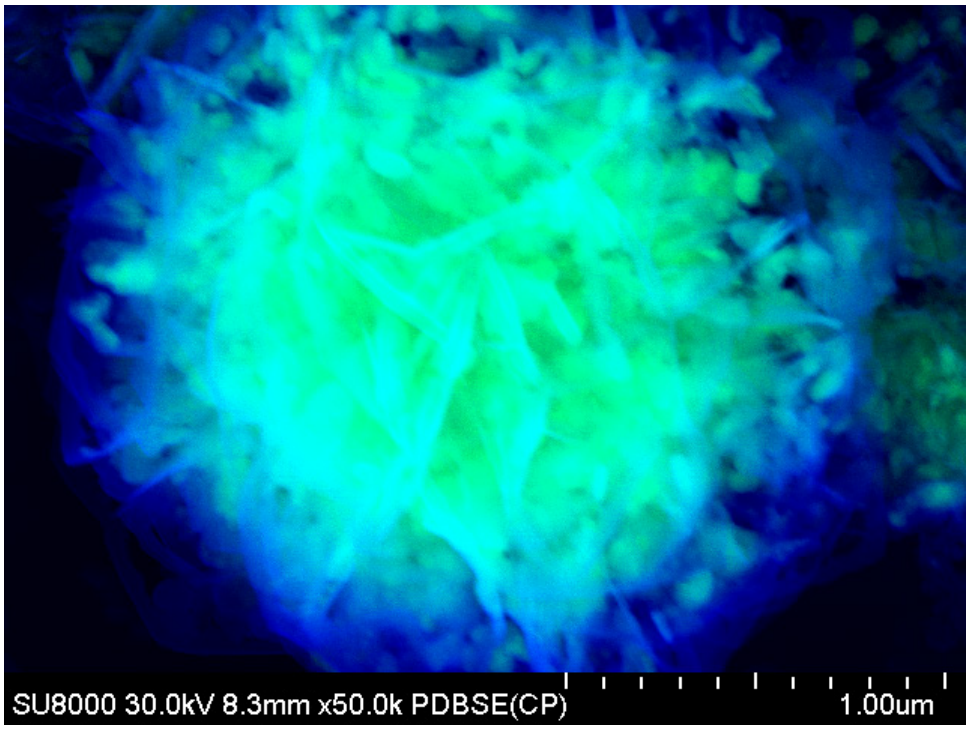

Figure S28. SEM image of catalyst after reduction at 400 °C (blue area – signal from SE detector, green-area – from PDBSE detector).

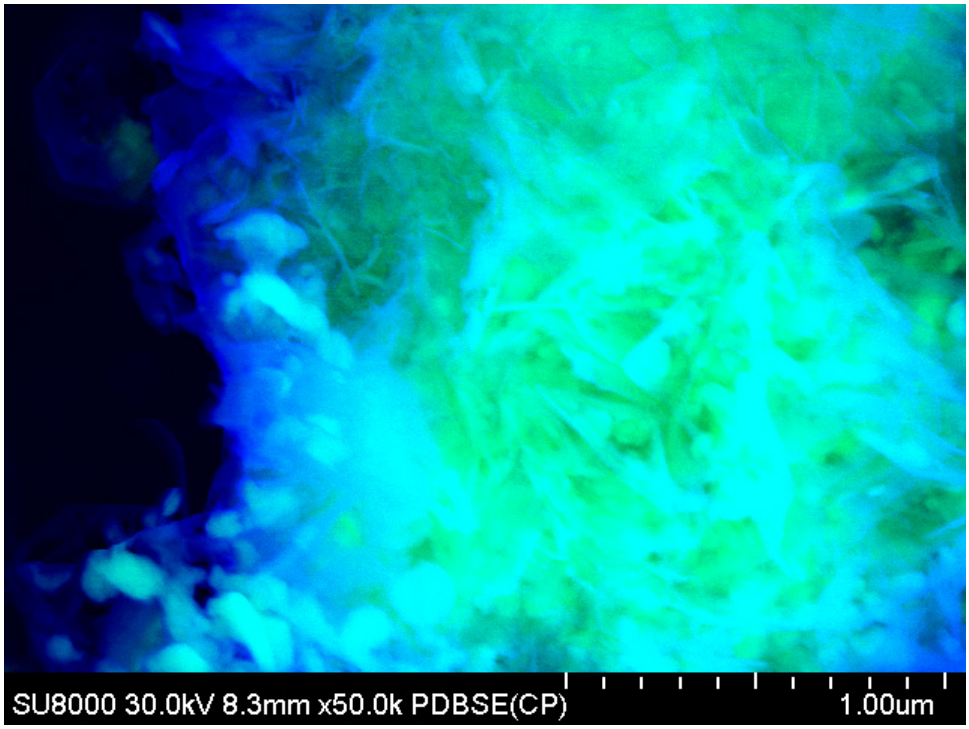

Figure S29. SEM image of catalyst after reduction at 400 °C (blue area – signal from SE detector, green-area – from PDBSE detector).

SEM images of catalyst after reduction at 600 ℃

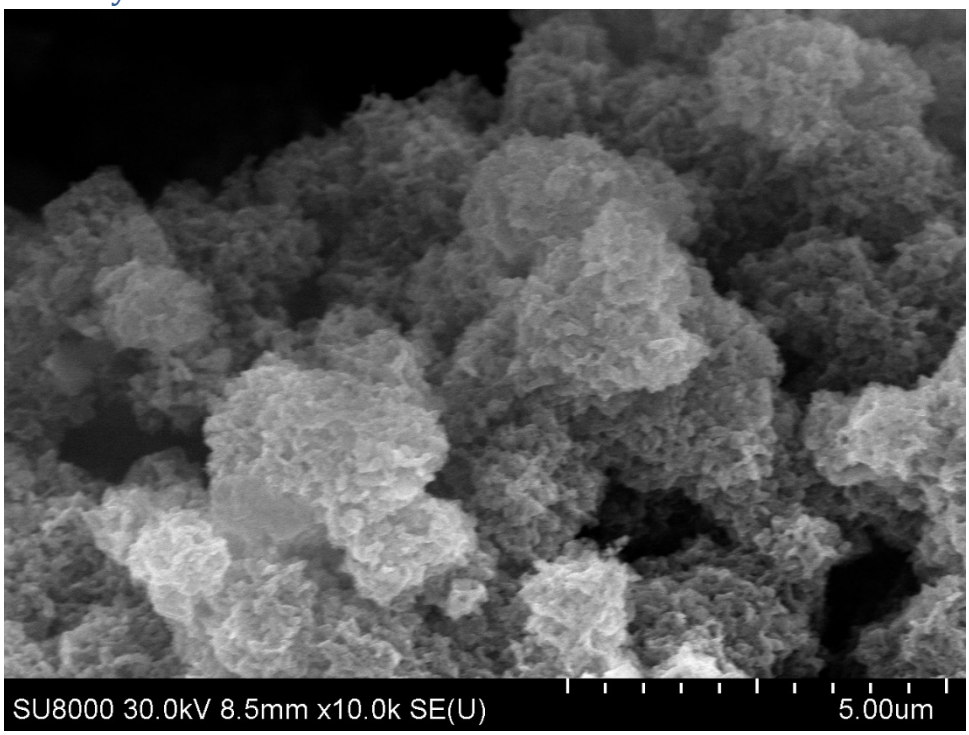

Figure S30. SEM image of catalyst after reduction at 600 ℃.

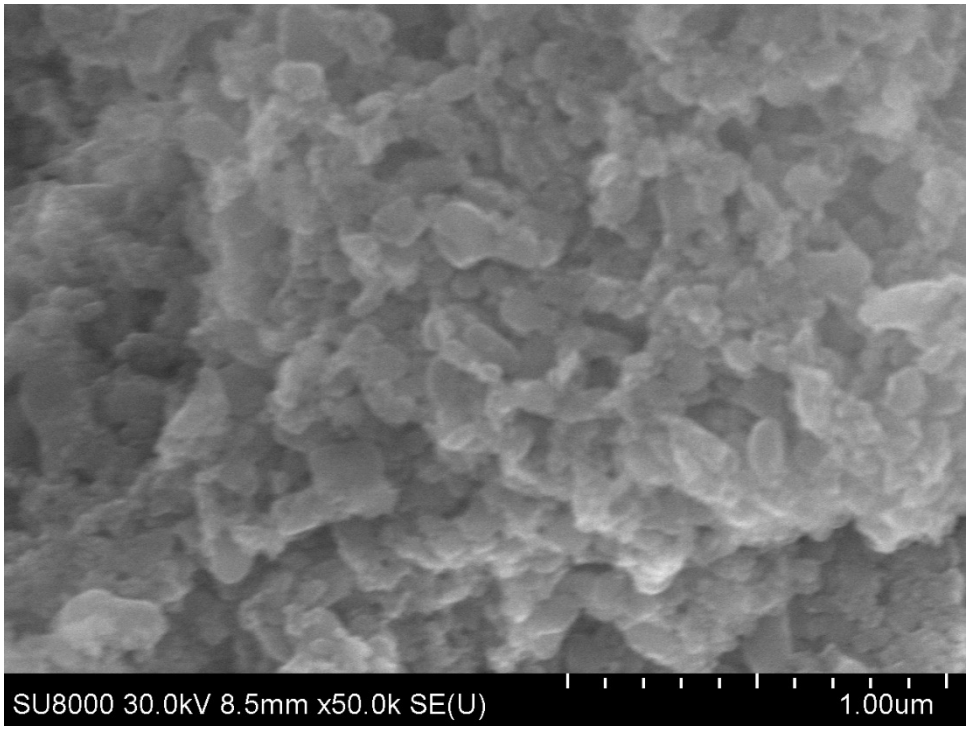

Figure S31. SEM image of catalyst after reduction at 600 ℃.

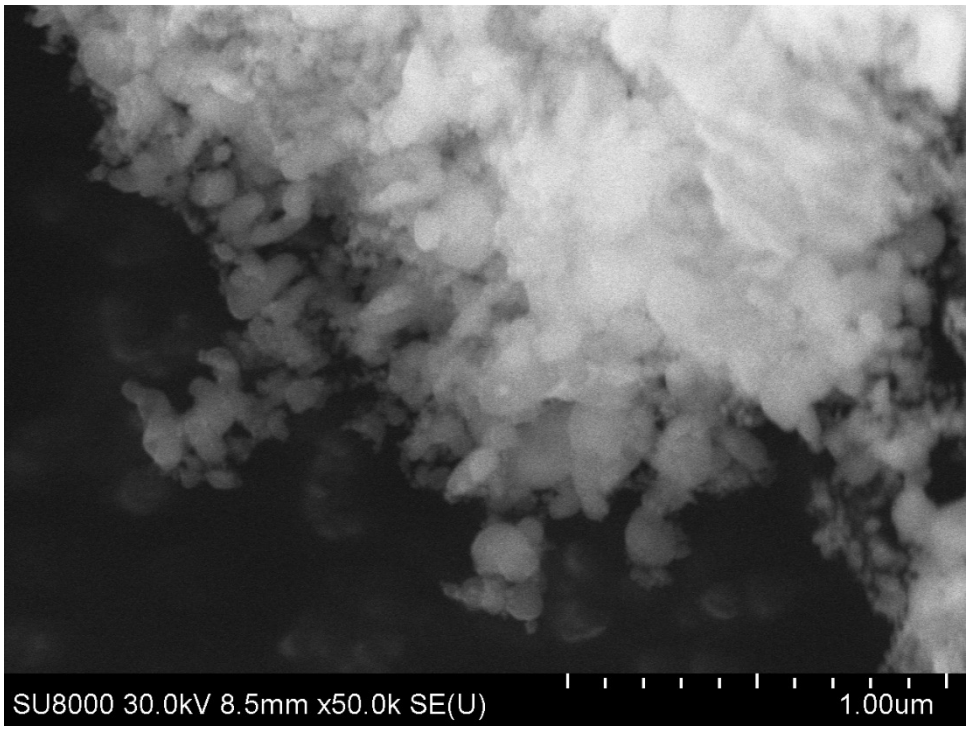

Figure S32. SEM image of catalyst after reduction at 600 ℃.

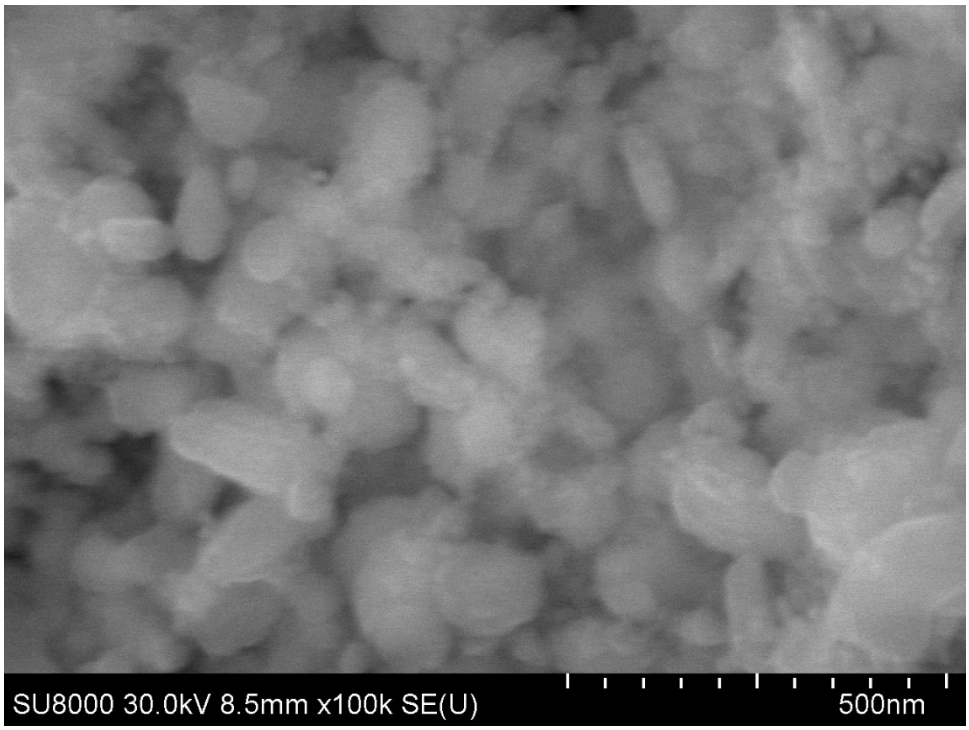

Figure S33. SEM image of catalyst after reduction at 600 ℃.

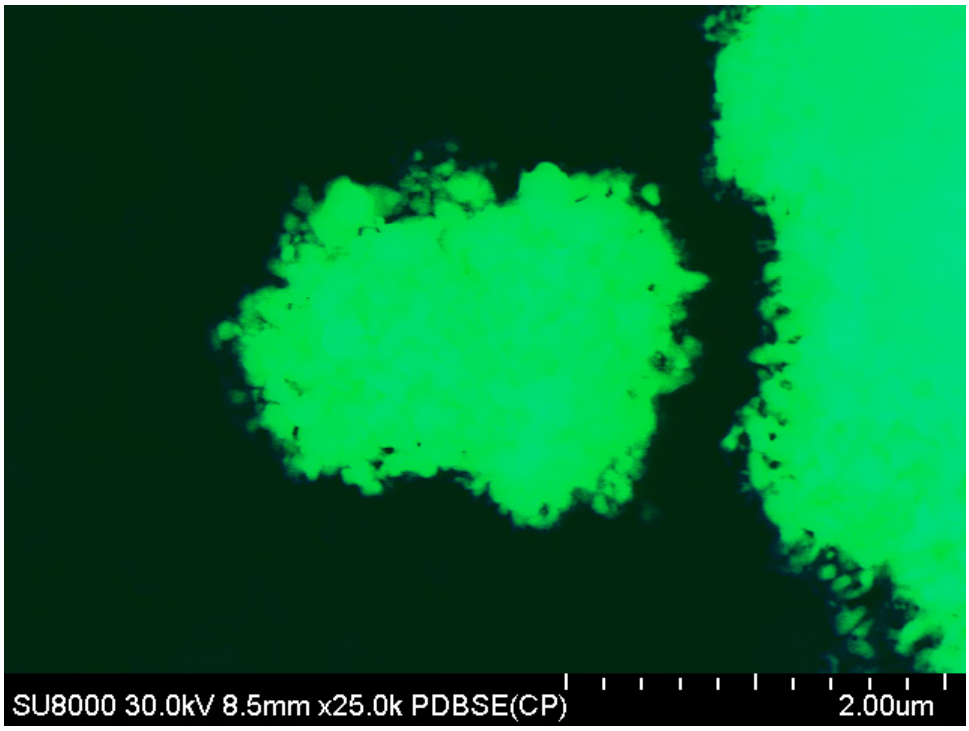

Figure S34. SEM image of catalyst after reduction at 600 °C (blue area – signal from SE detector, green-area – from PDBSE detector).

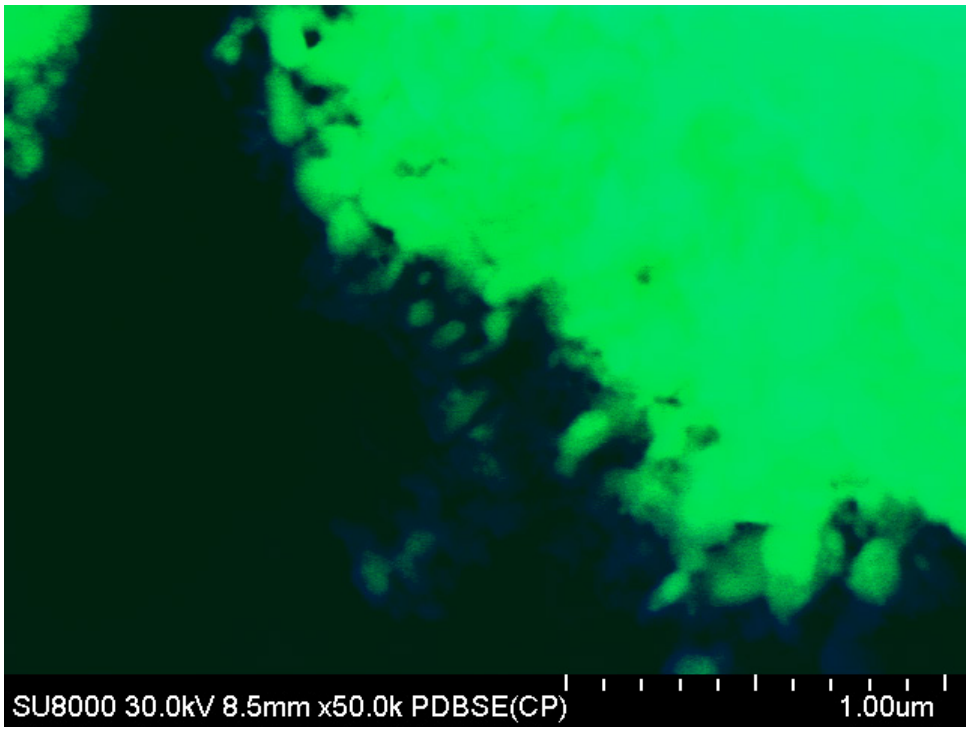

Figure S35. SEM image of catalyst after reduction at 600 °C (blue area – signal from SE detector, green-area – from PDBSE detector).

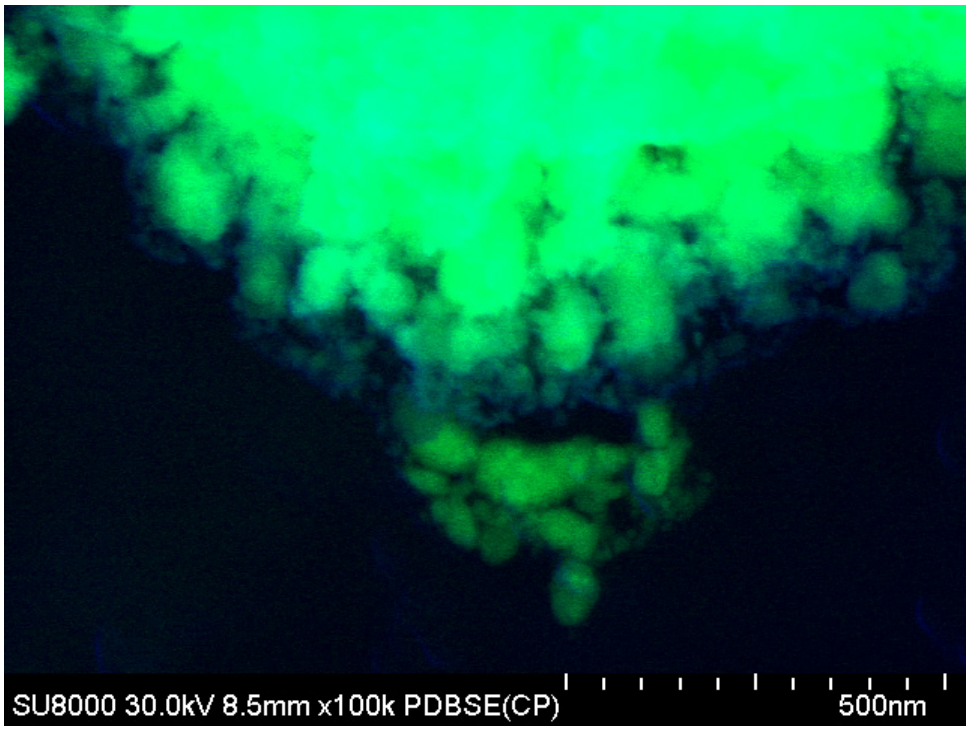

Figure S36. SEM image of catalyst after reduction at 600 ℃ (blue area – signal from SE detector, green-area – from PDBSE detector).

EDS of catalyst before reduction

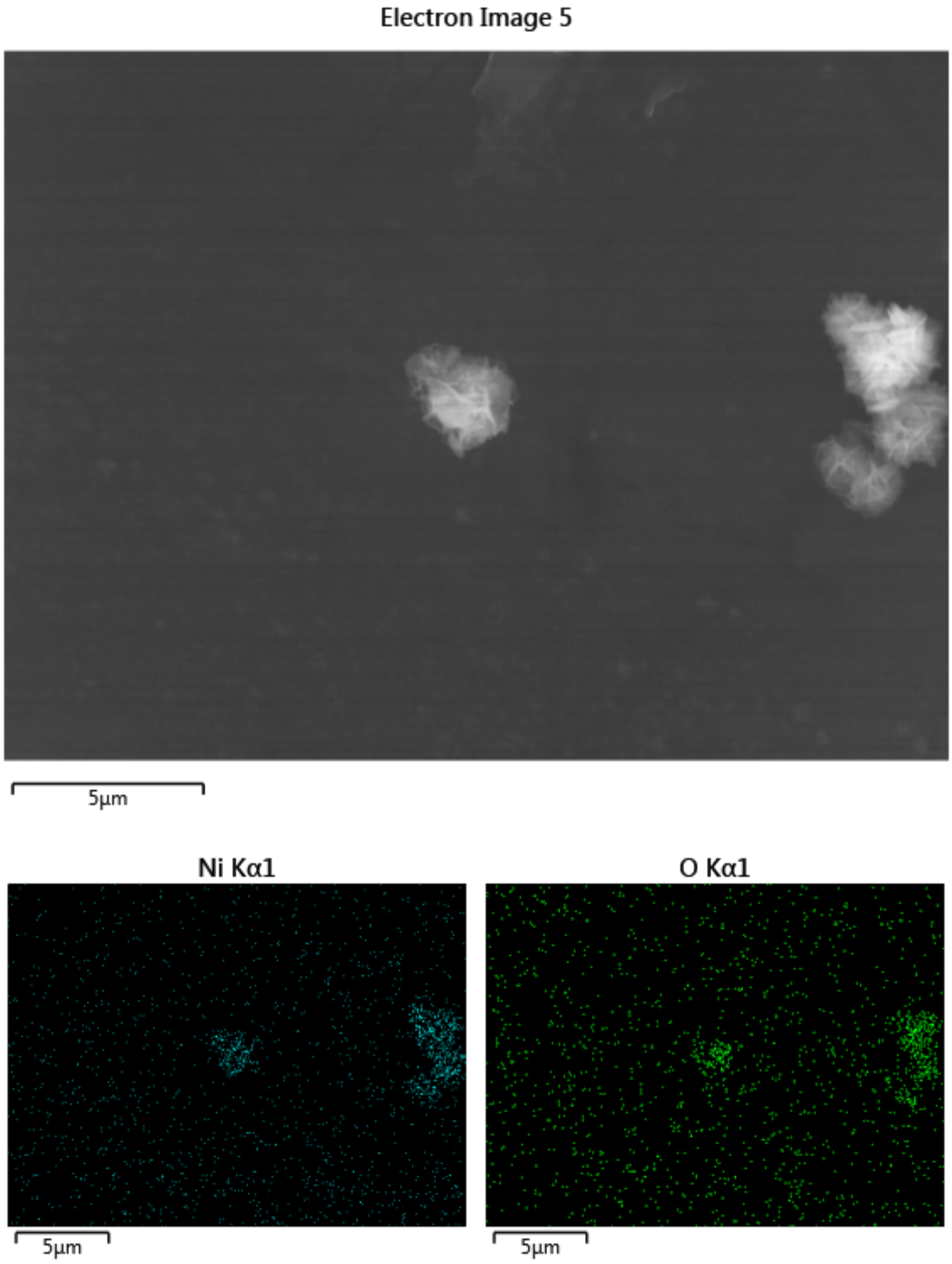

Figure S37. SEM image and EDS elements distribution maps of catalyst before reduction.

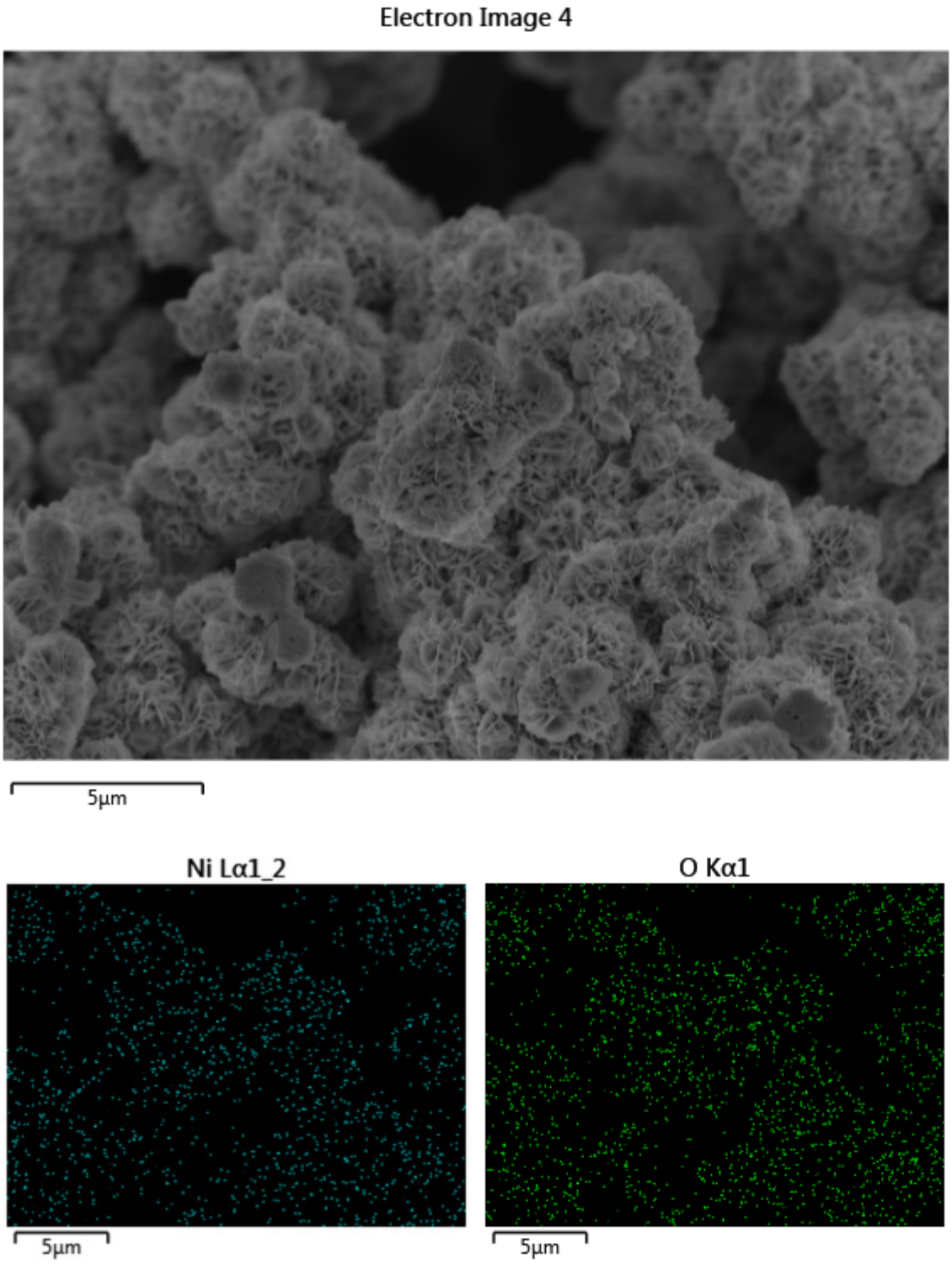

Figure S38. SEM image and EDS elements distribution maps of catalyst before reduction.

EDS of catalyst after reduction

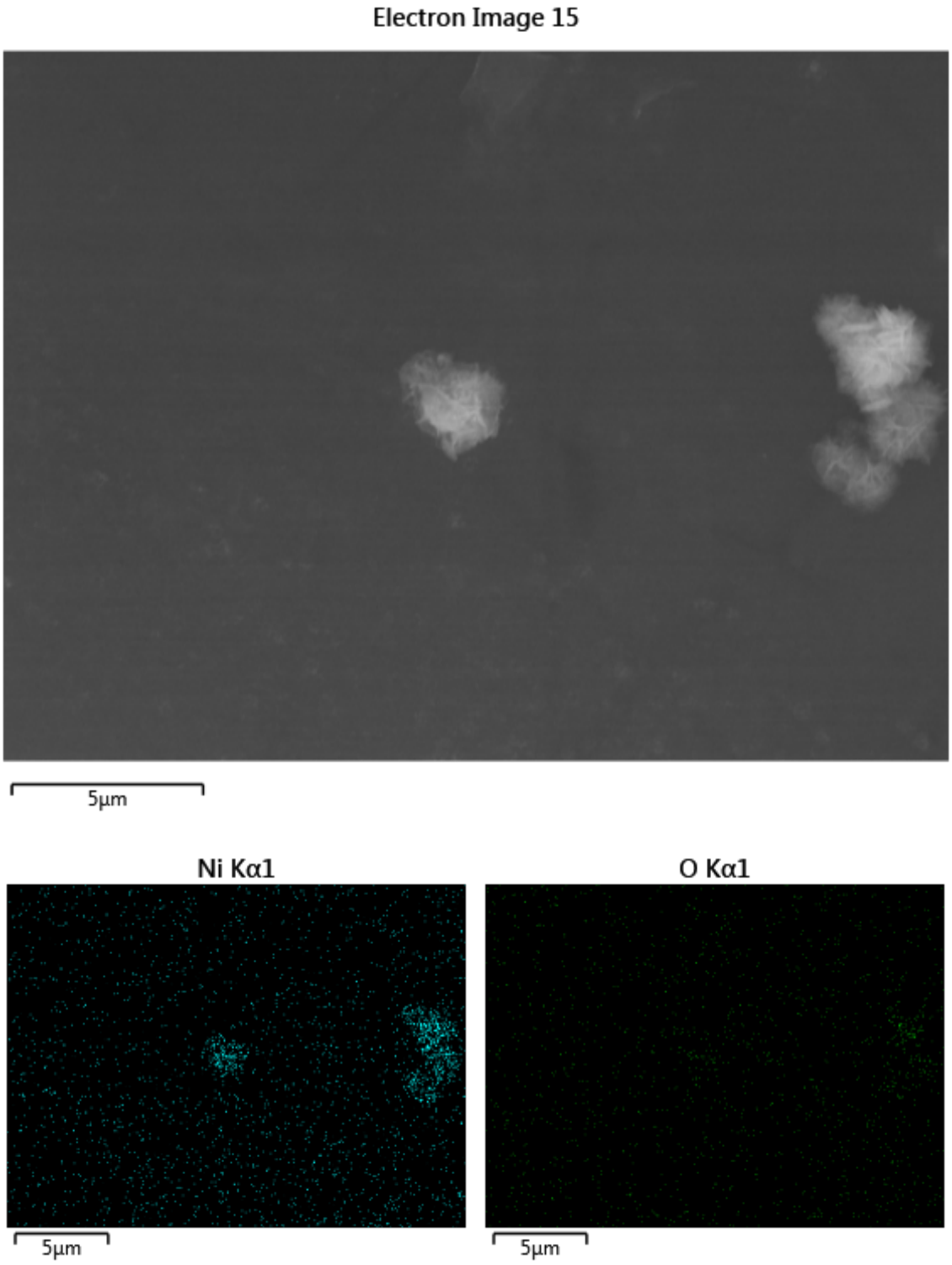

Figure S39. SEM image and EDS elements distribution maps of catalyst after reduction at 400 ℃.

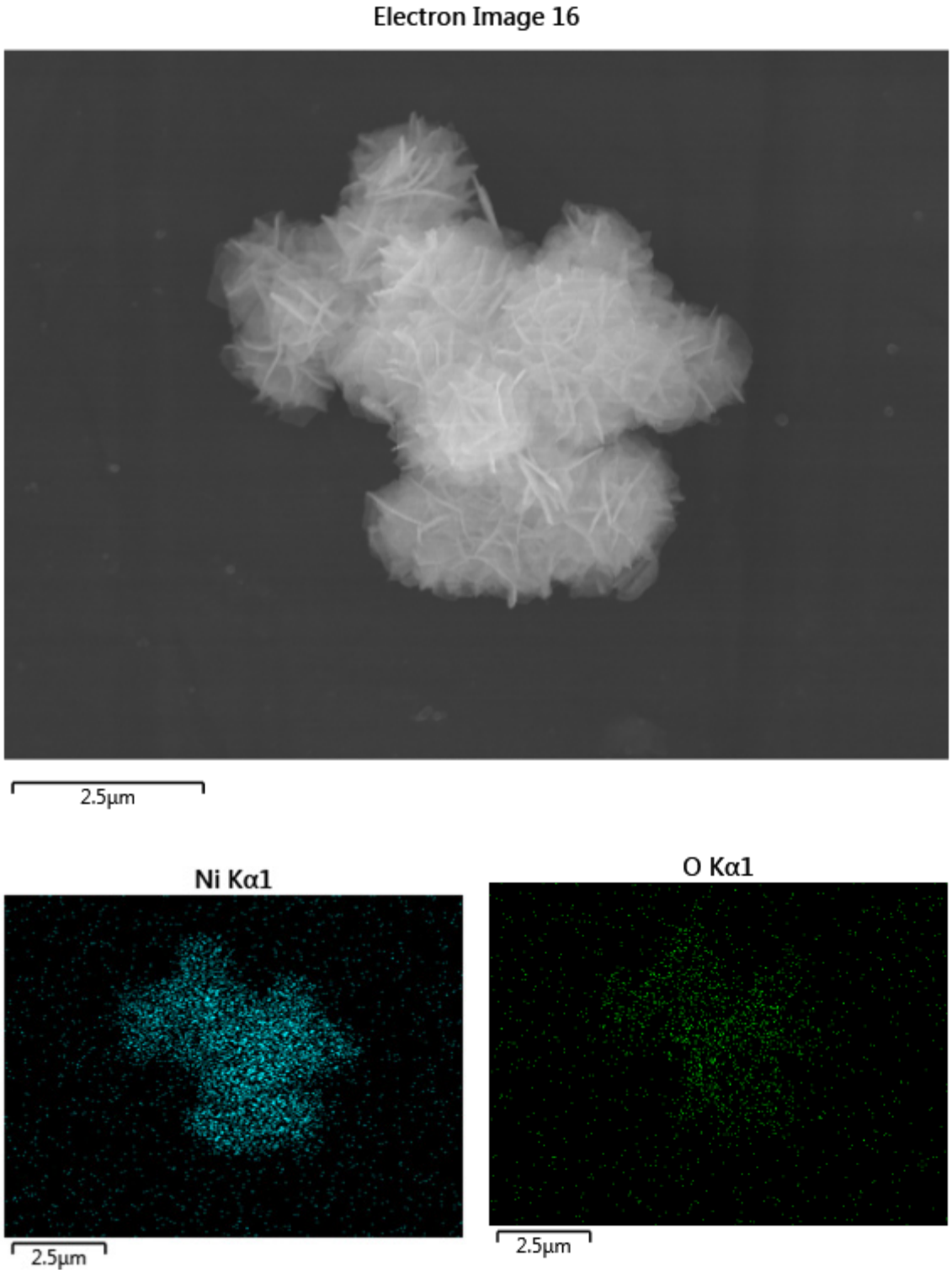

Figure S40. SEM image and EDS elements distribution maps of catalyst after reduction at 400 °C.

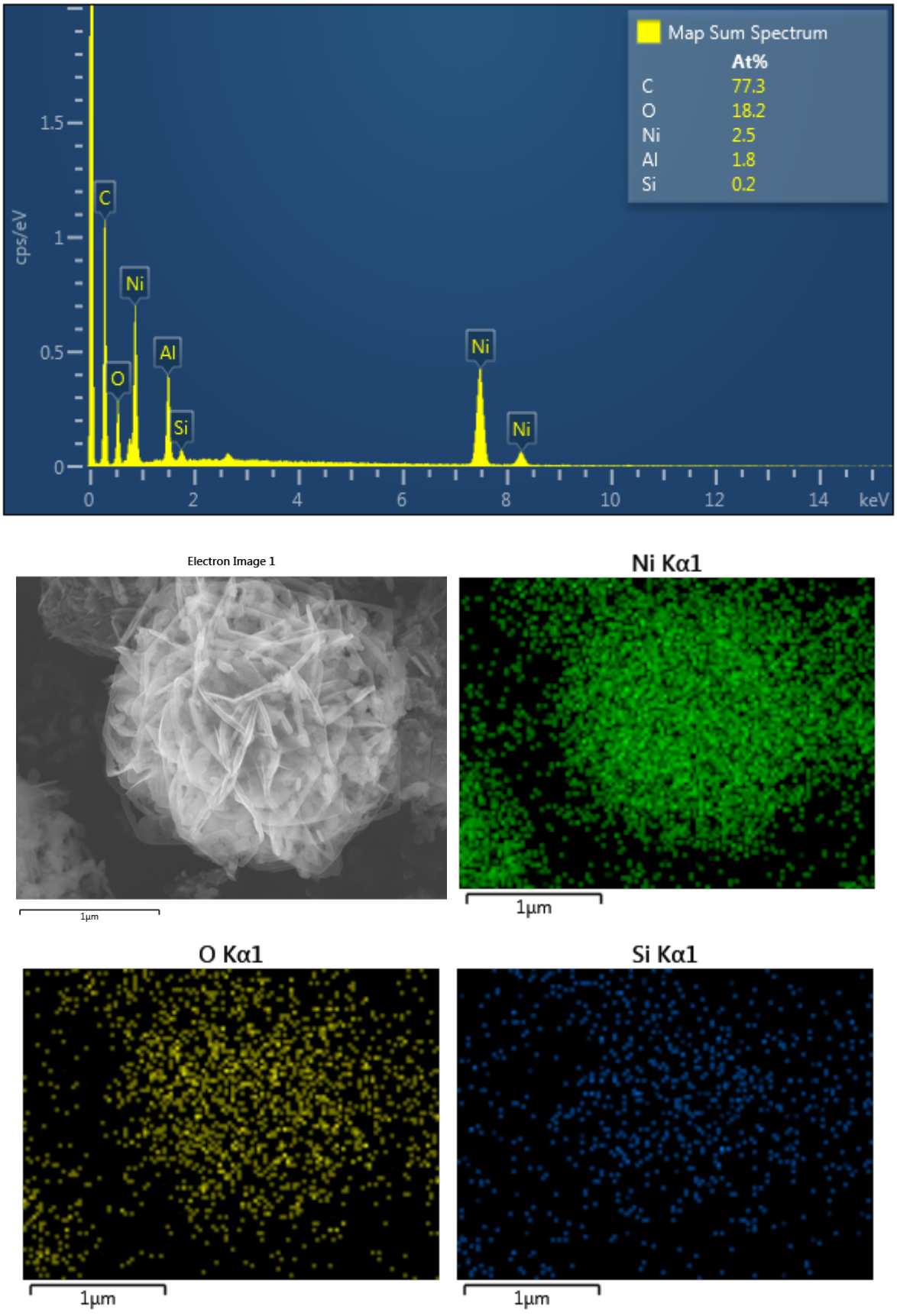

Figure S41. SEM image and EDS elements distribution maps of catalyst after reduction at 400 °C.

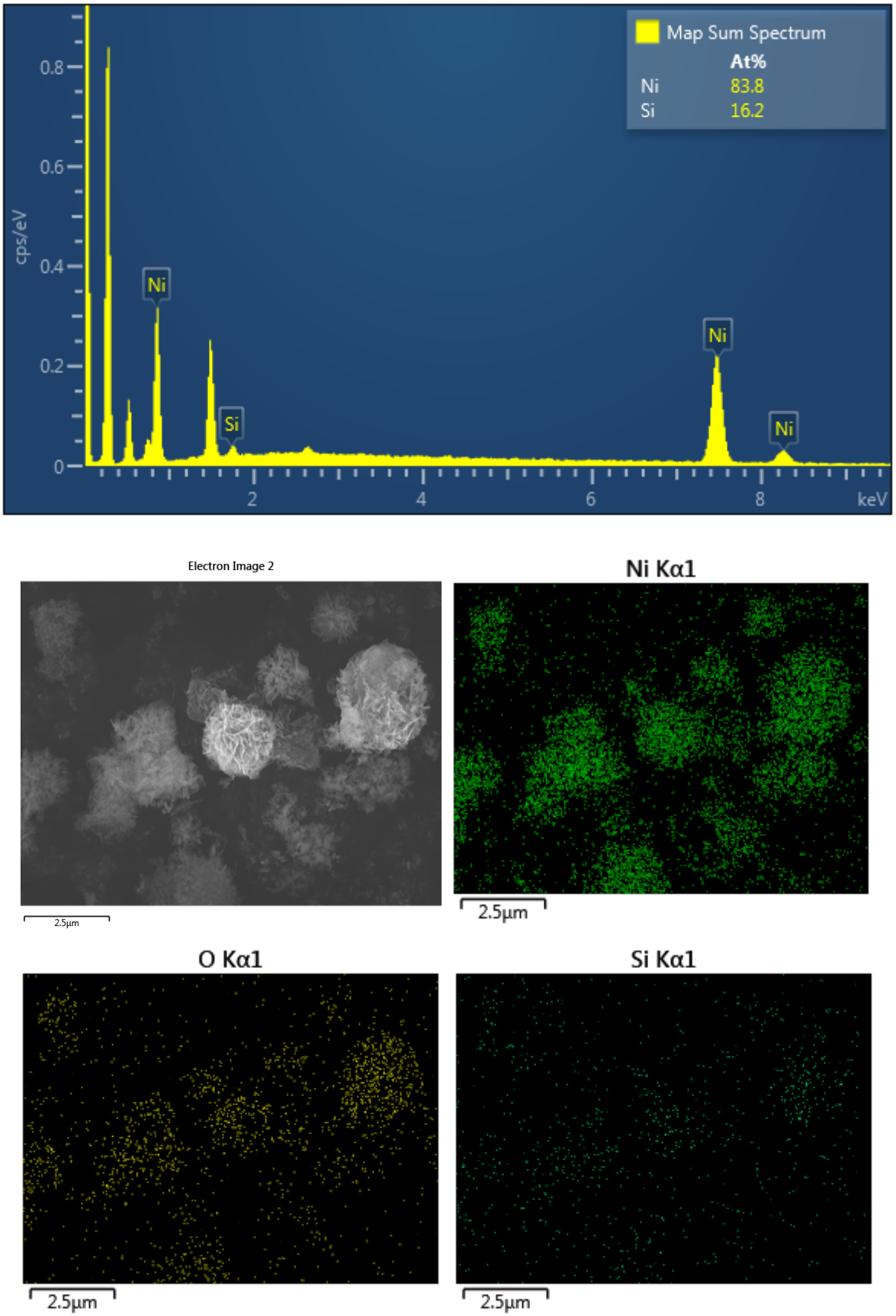

Figure S42. SEM image and EDS elements distribution maps of catalyst after reduction at 400 ℃.

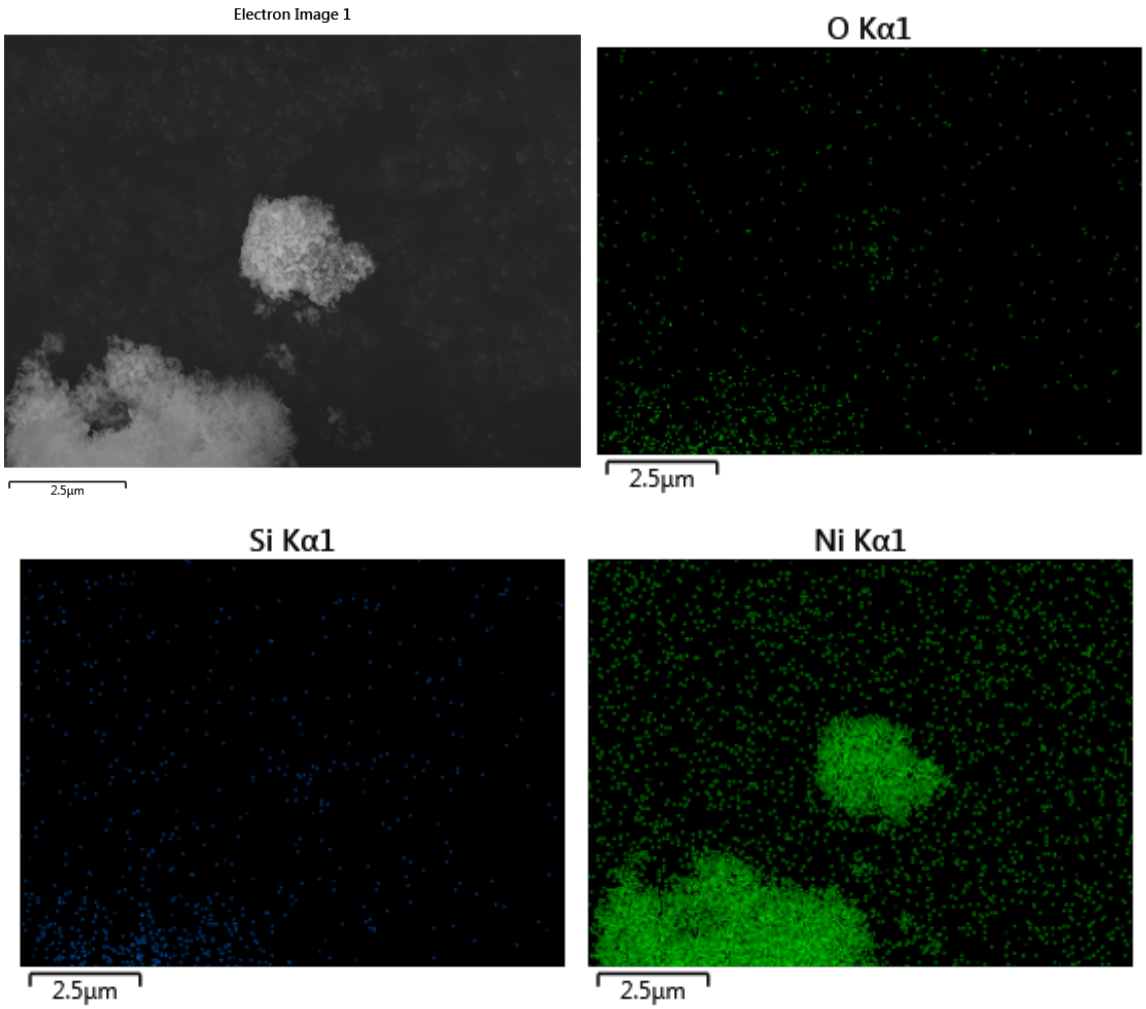

Figure S43. SEM image and EDS elements distribution maps of catalyst after reduction at 600 ℃.

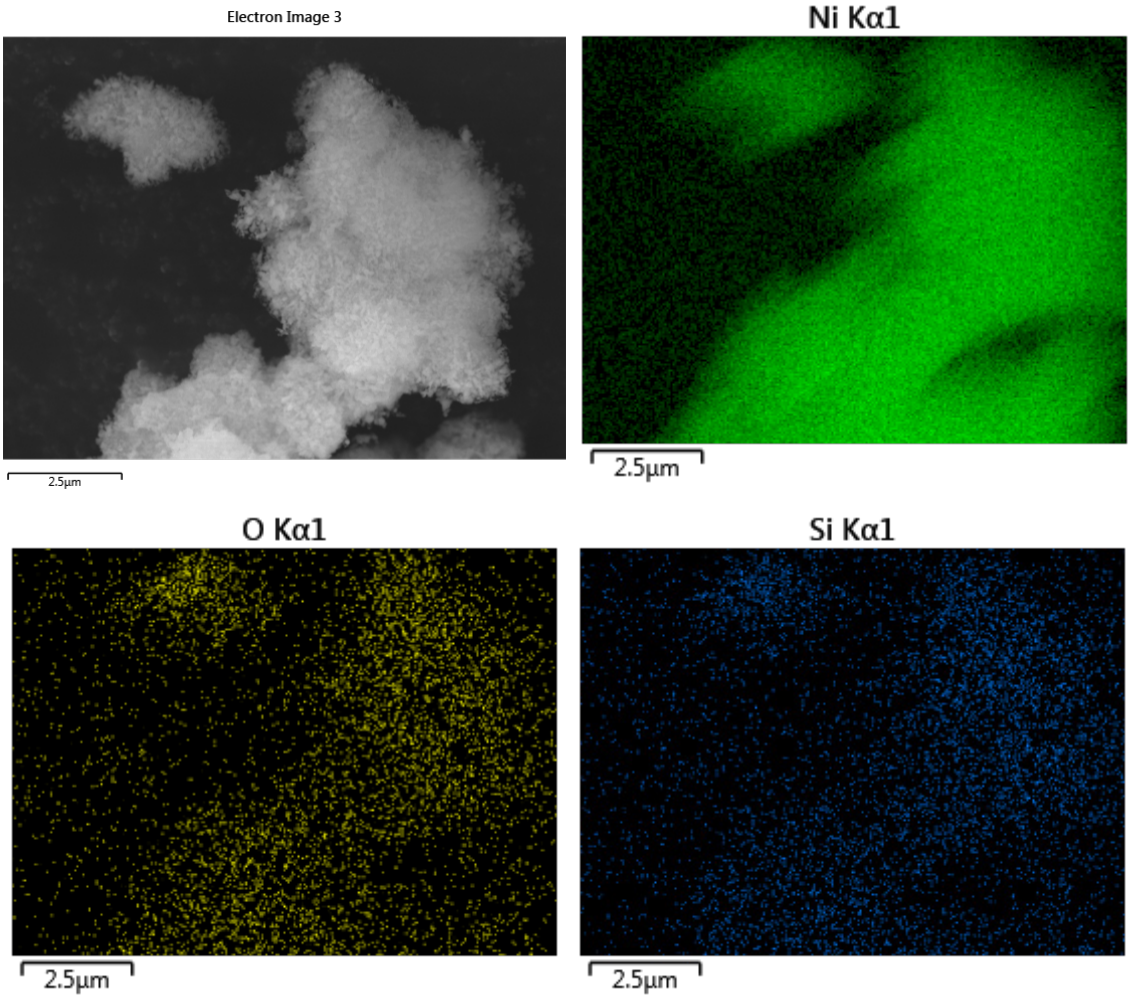

Figure S44. SEM image and EDS elements distribution maps of catalyst after reduction at 600 °C.

TEM images of catalyst after reduction at 400 ℃

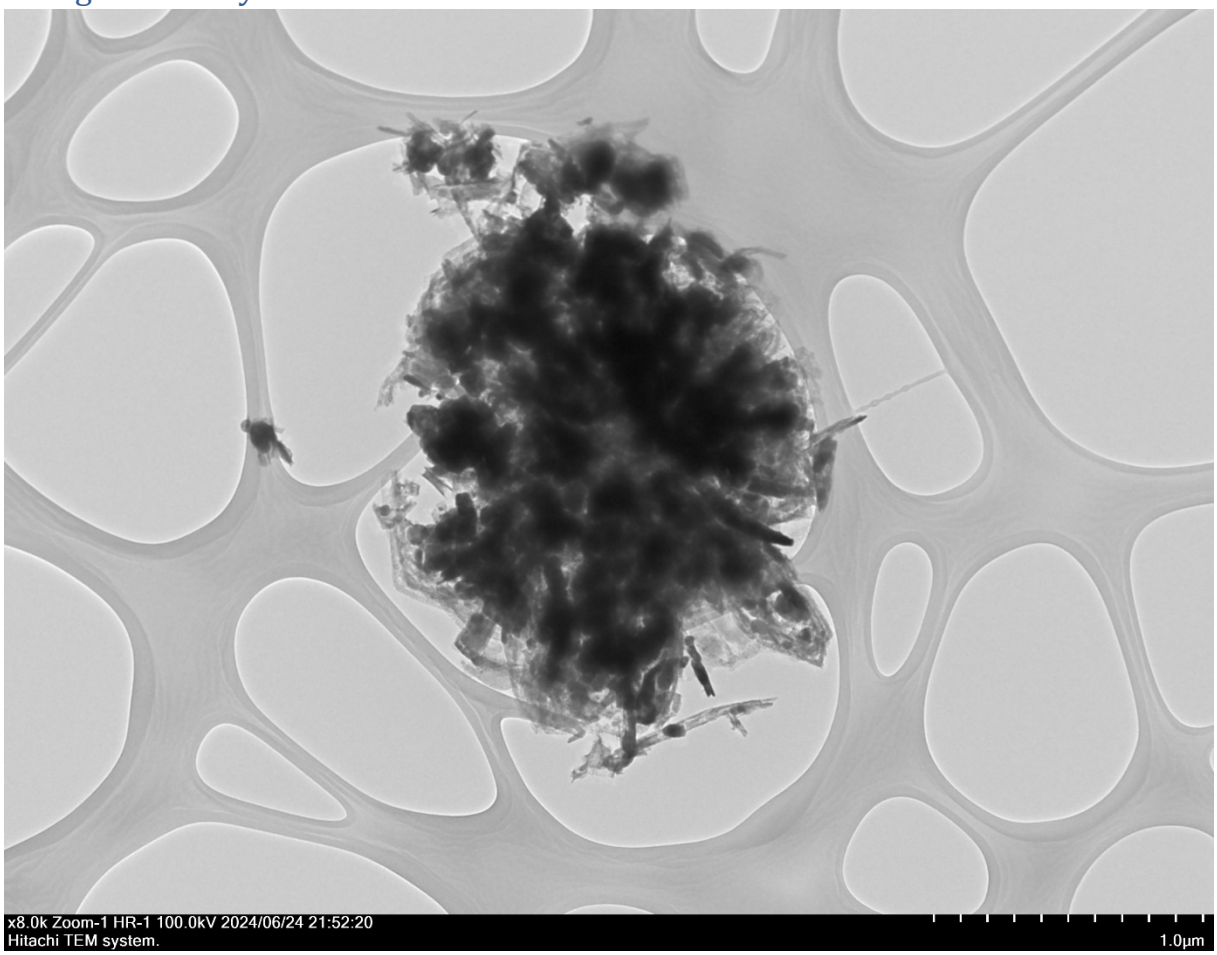

Figure S45. TEM image of catalyst after reduction at 400 ℃.

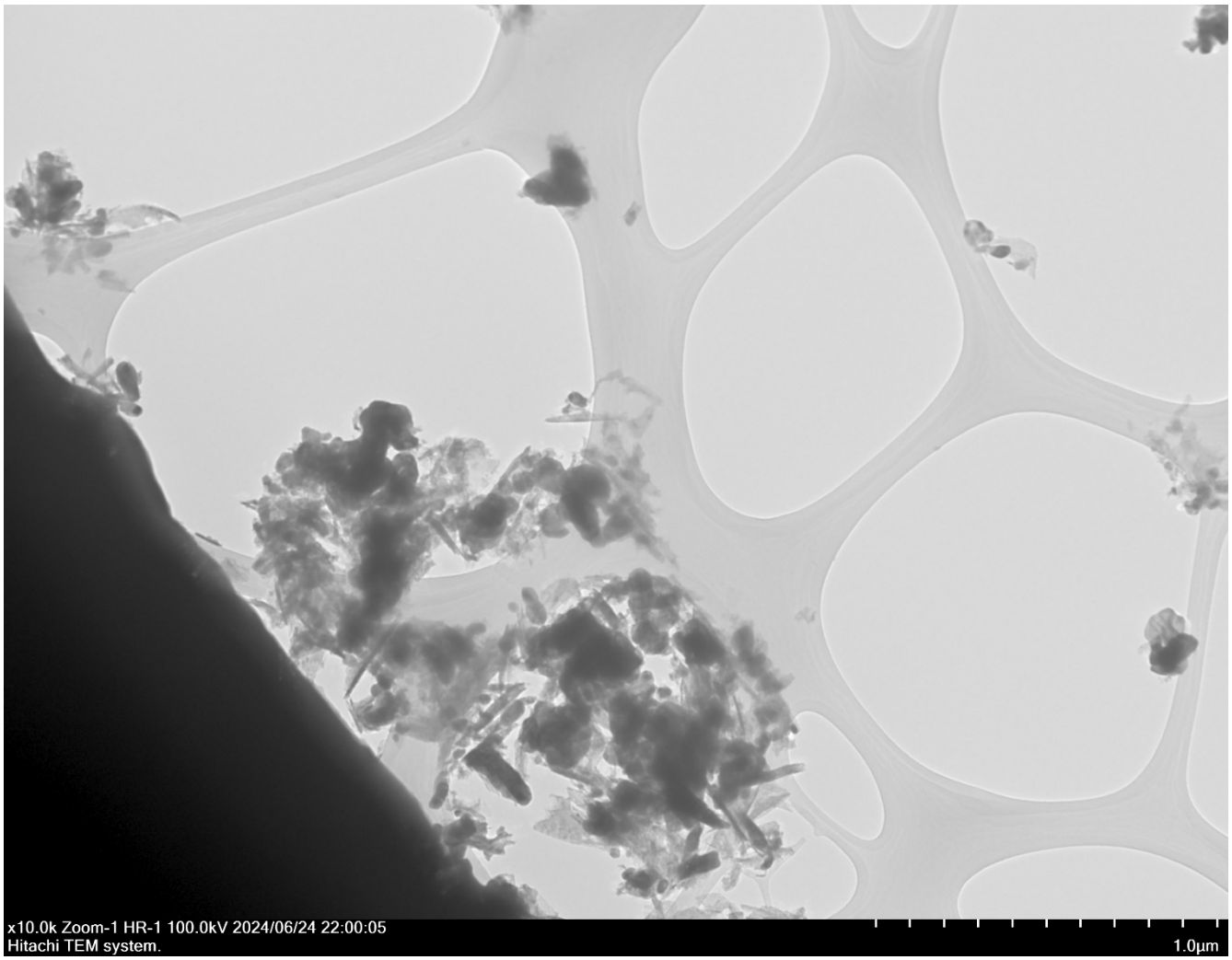

Figure S46. TEM image of catalyst after reduction at 400 ℃.

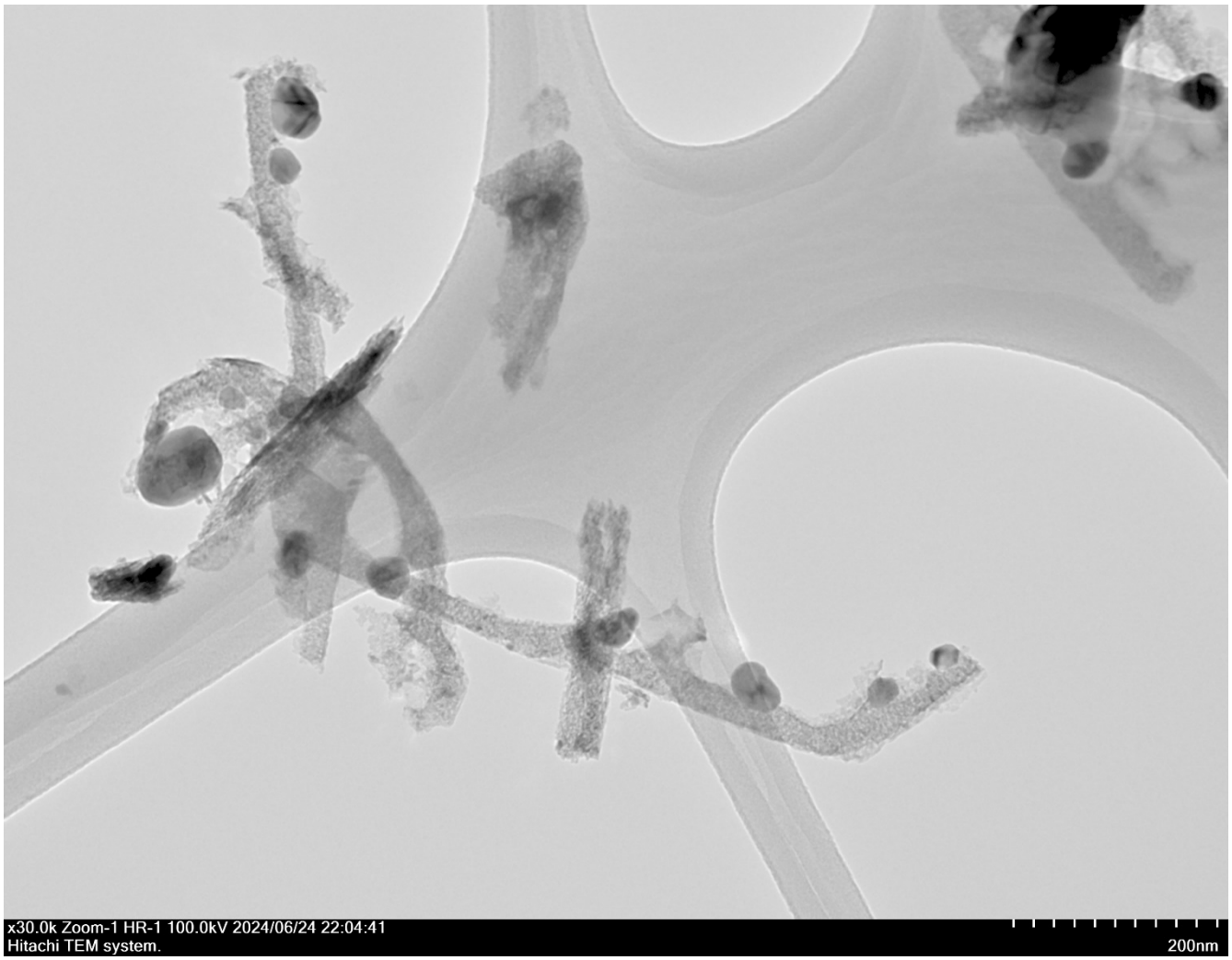

Figure S47. TEM image of catalyst after reduction at 400 ℃.

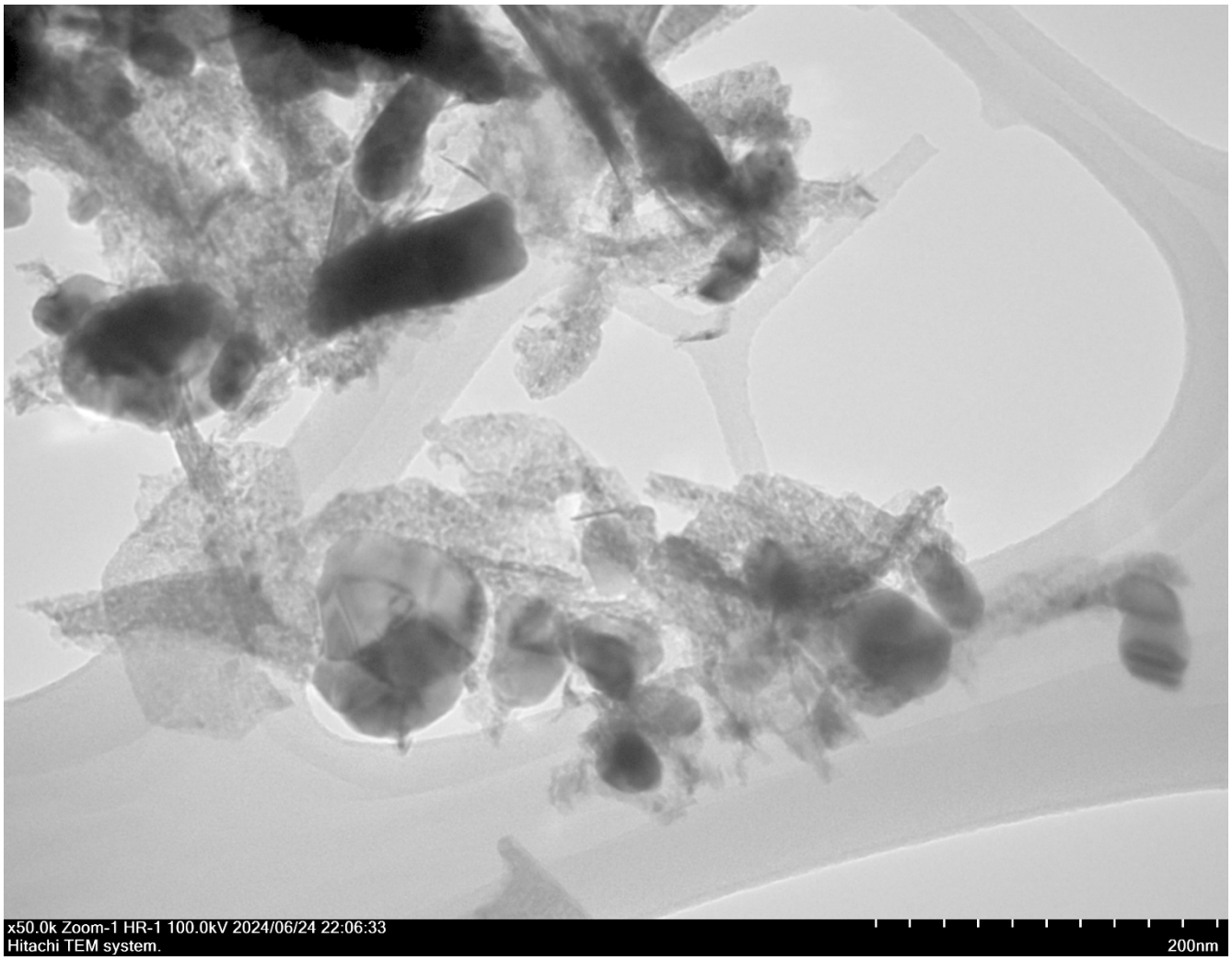

Figure S48. TEM image of catalyst after reduction at 400 ℃.

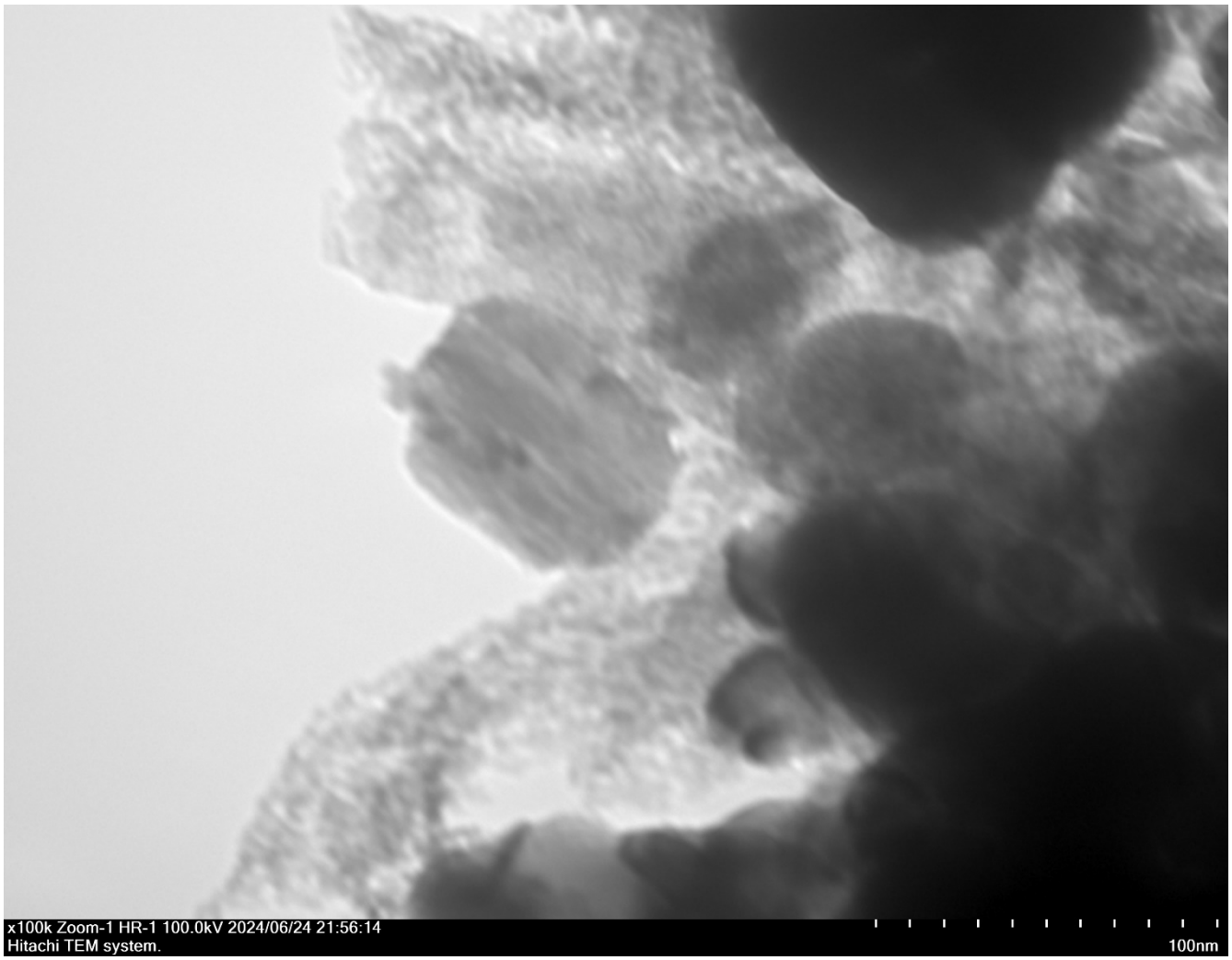

Figure S49. TEM image of catalyst after reduction at 400 ℃.

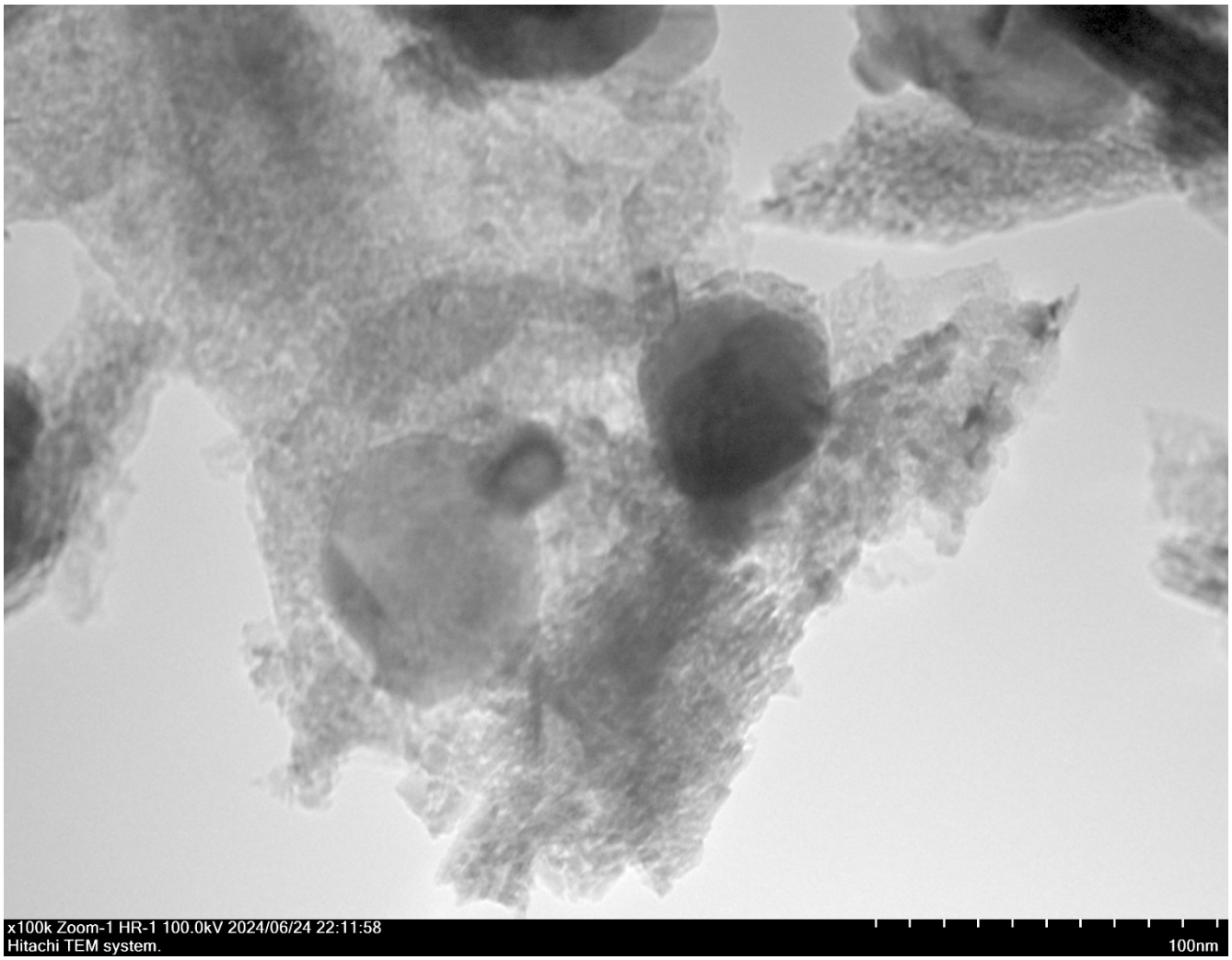

Figure S50. TEM image of catalyst after reduction at 400 ℃.

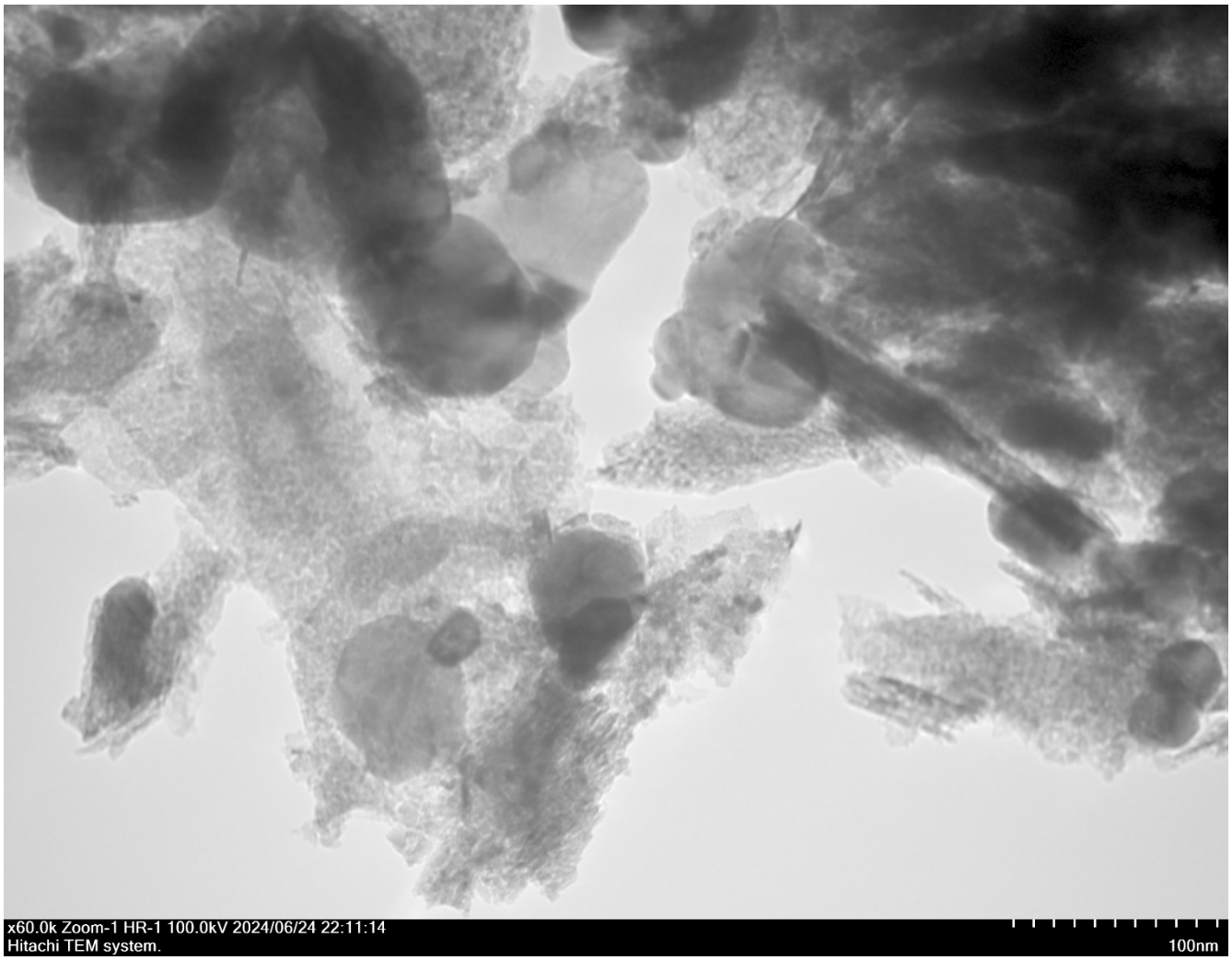

Figure S51. TEM image of catalyst after reduction at 400 ℃.

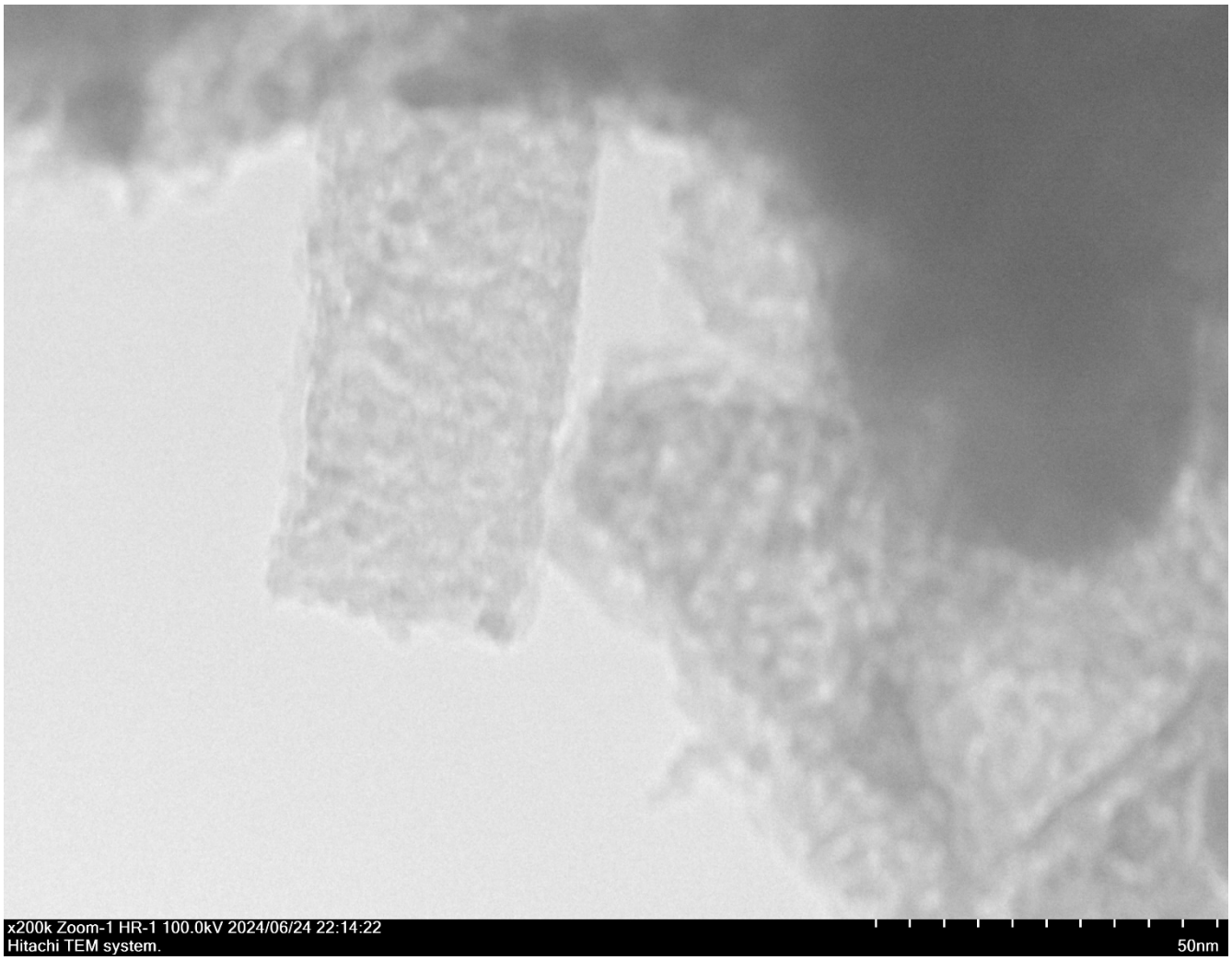

Figure S52. TEM image of catalyst after reduction at 400 ℃.

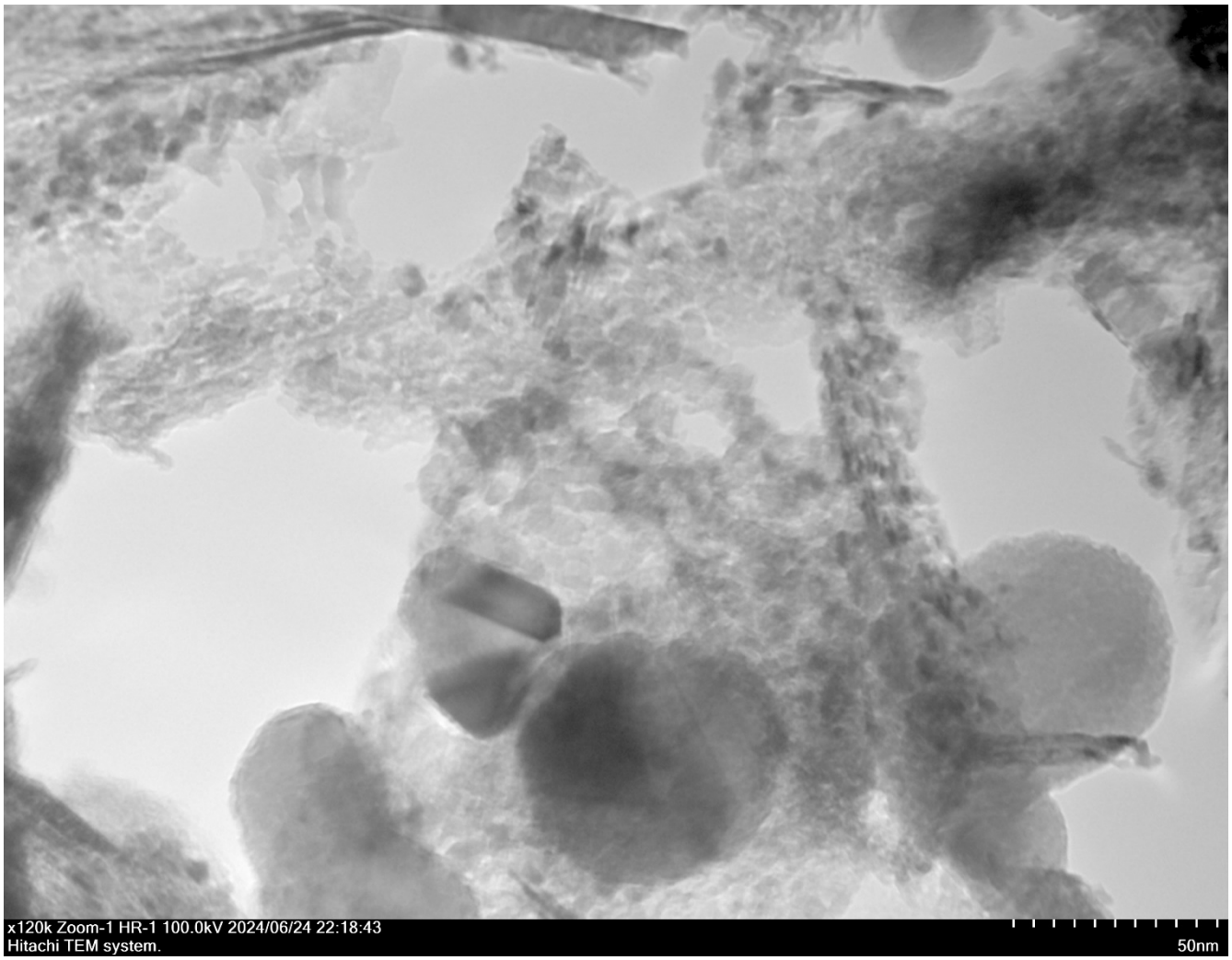

Figure S53. TEM image of catalyst after reduction at 400 ℃.

TEM images of catalyst after reduction at 600 ℃

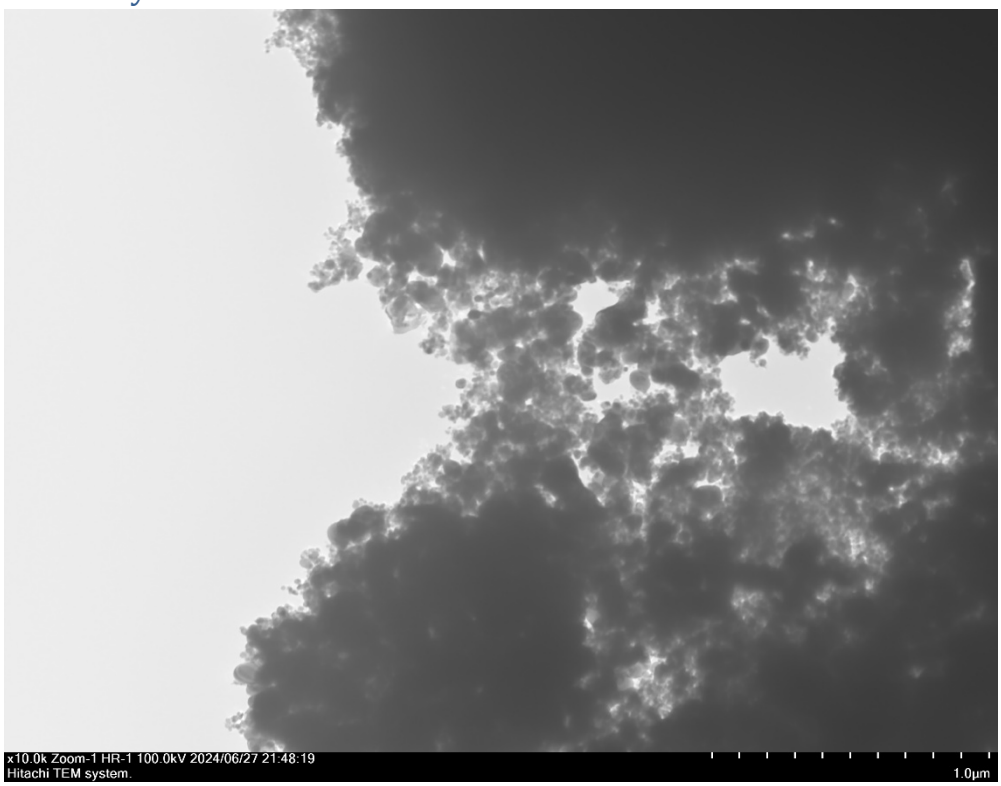

Figure S54. TEM image of catalyst after reduction at 600 ℃.

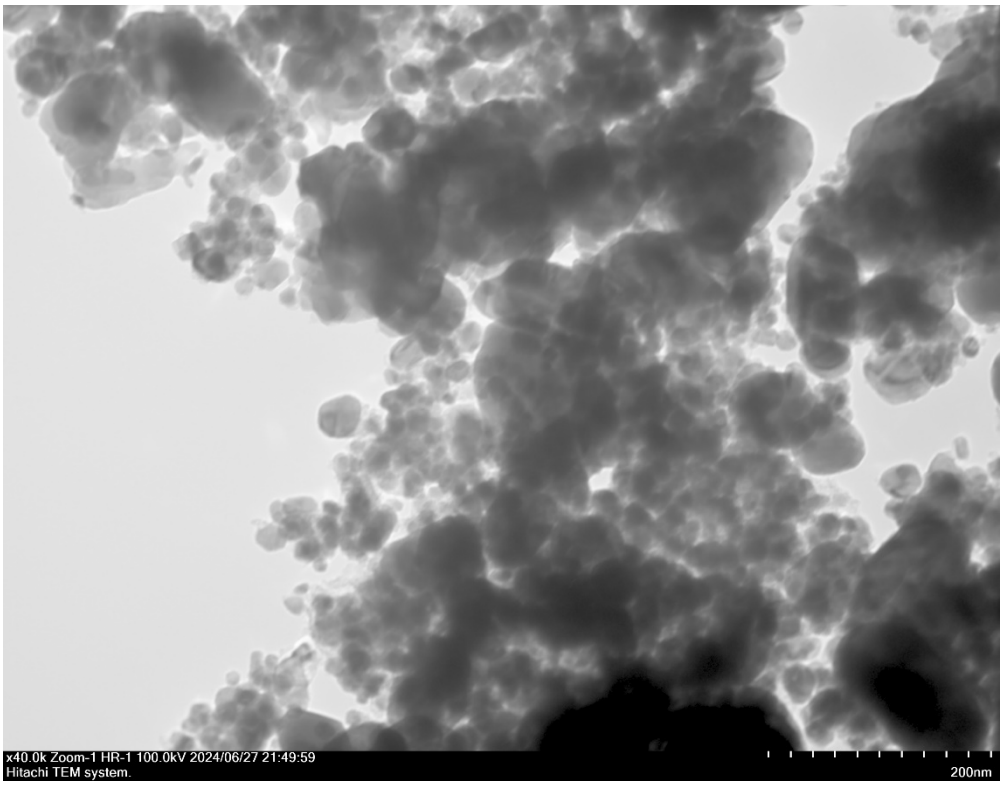

Figure S55. TEM image of catalyst after reduction at 600 ℃.

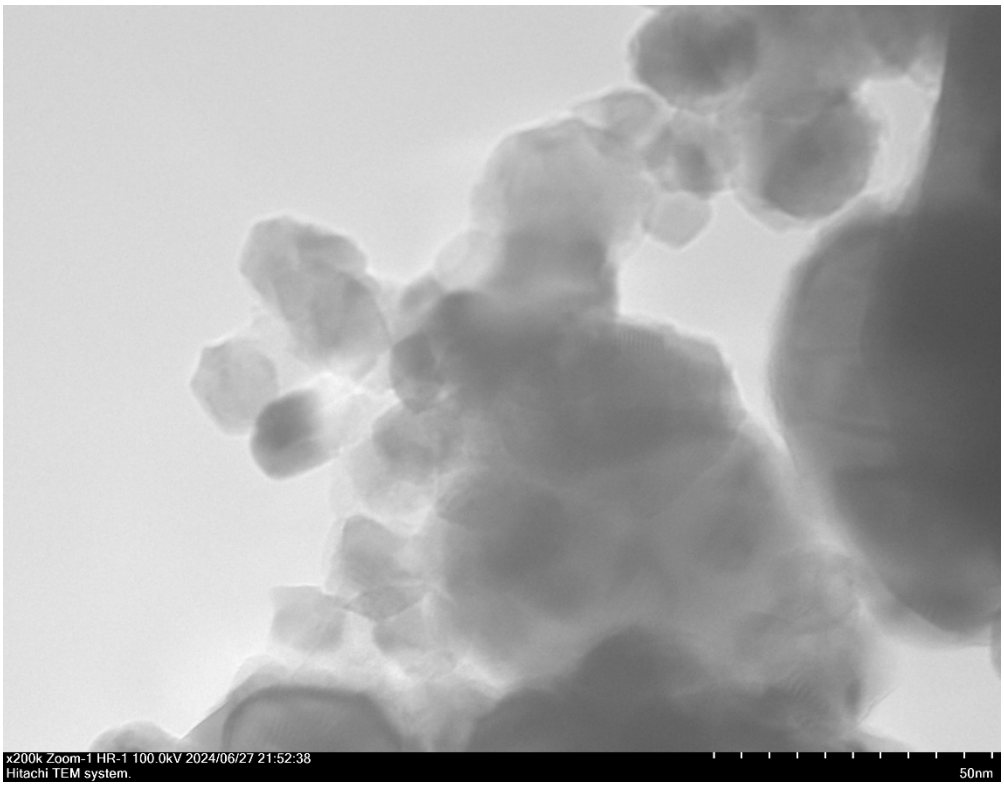

Figure S56. TEM image of catalyst after reduction at 600 ℃.

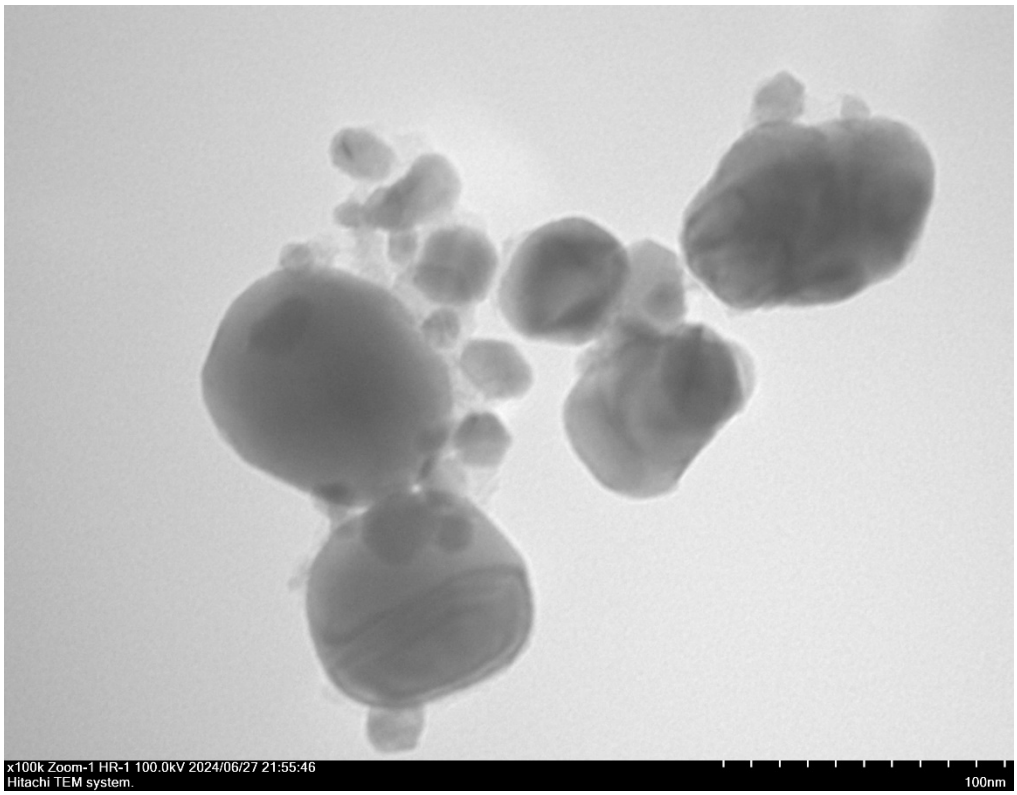

Figure S57. TEM image of catalyst after reduction at 600 ℃.

Particle size distribution

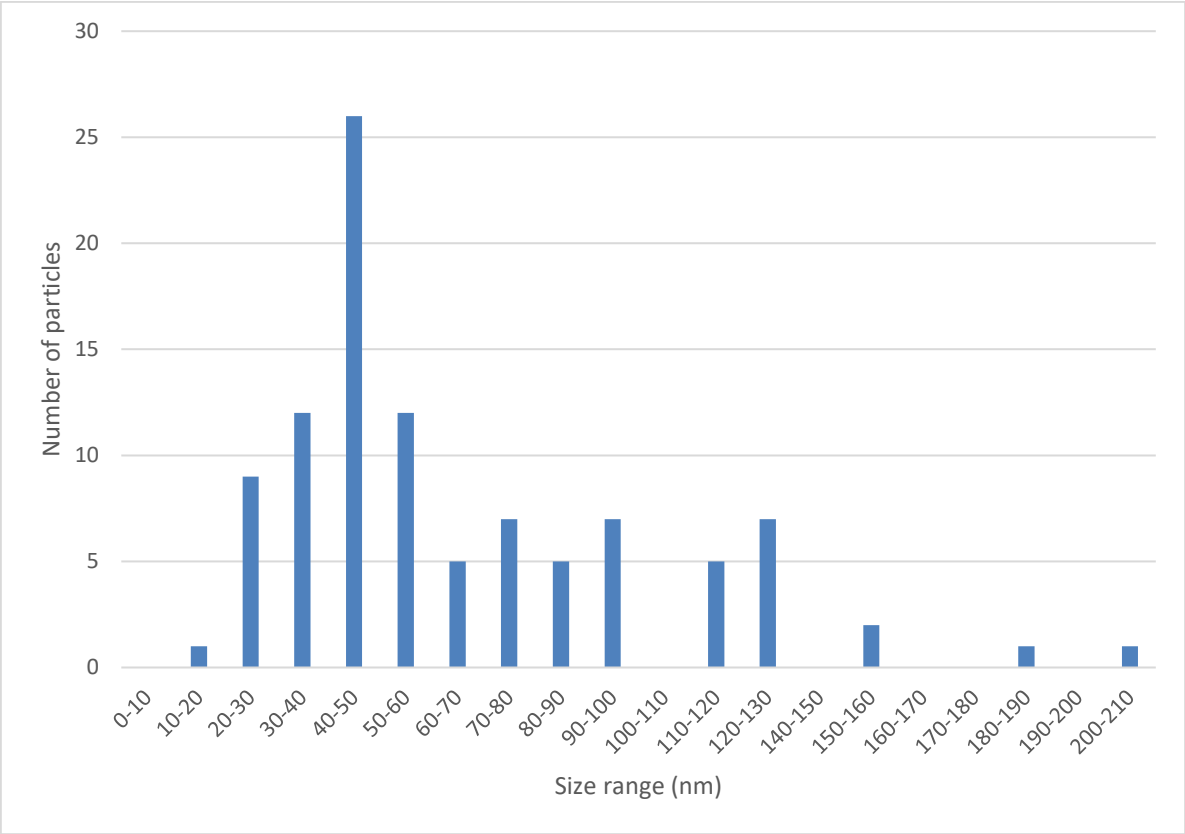

Figure S58. Particle size distribution after reduction at 400 °C (calculated from TEM images).

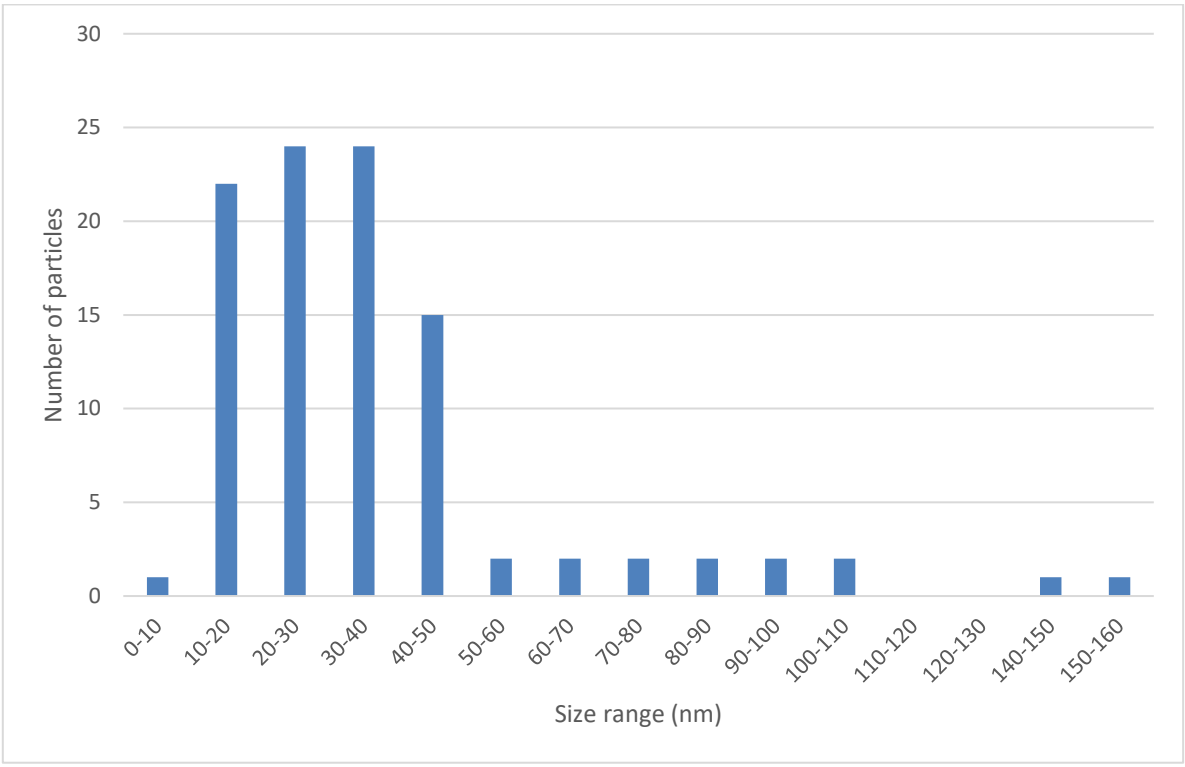

Figure S59. Particle size distribution after reduction at 600 °C (calculated from TEM images).

XRD of catalysts

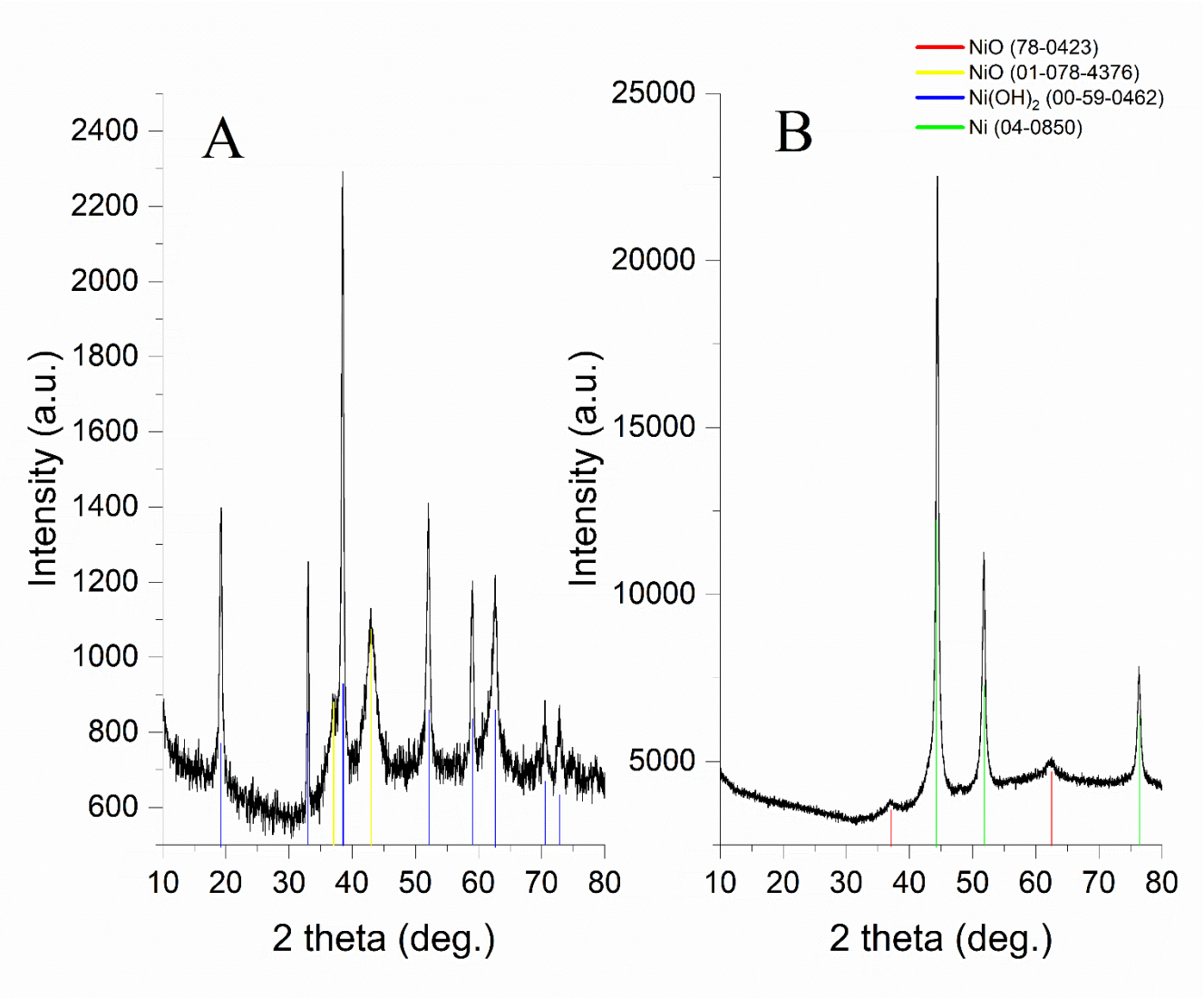

Figure S60. XRD of catalyst before (A) and after (B) reduction at 400 ℃.

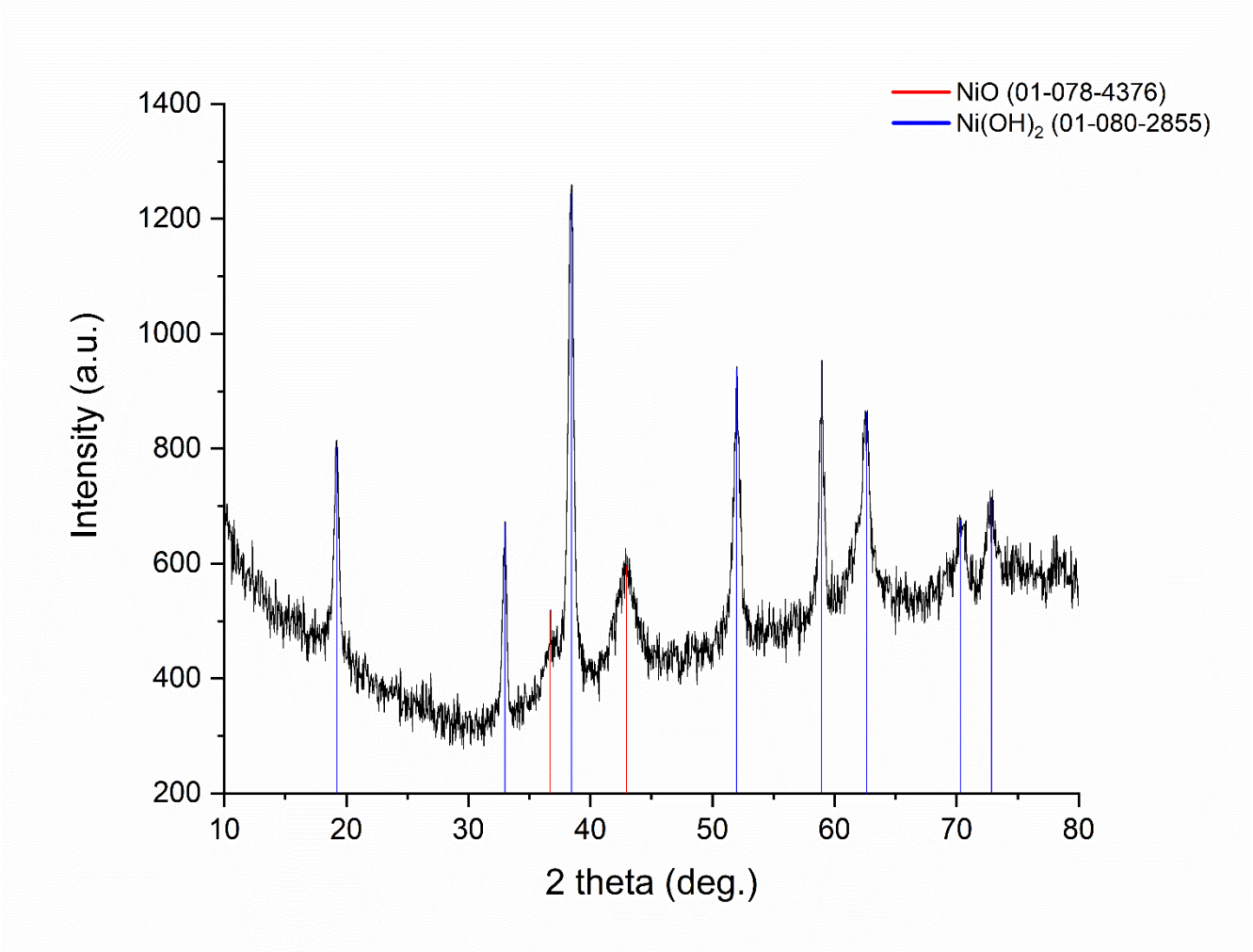

Figure S61. XRD of catalyst after reduction at 200 ℃.

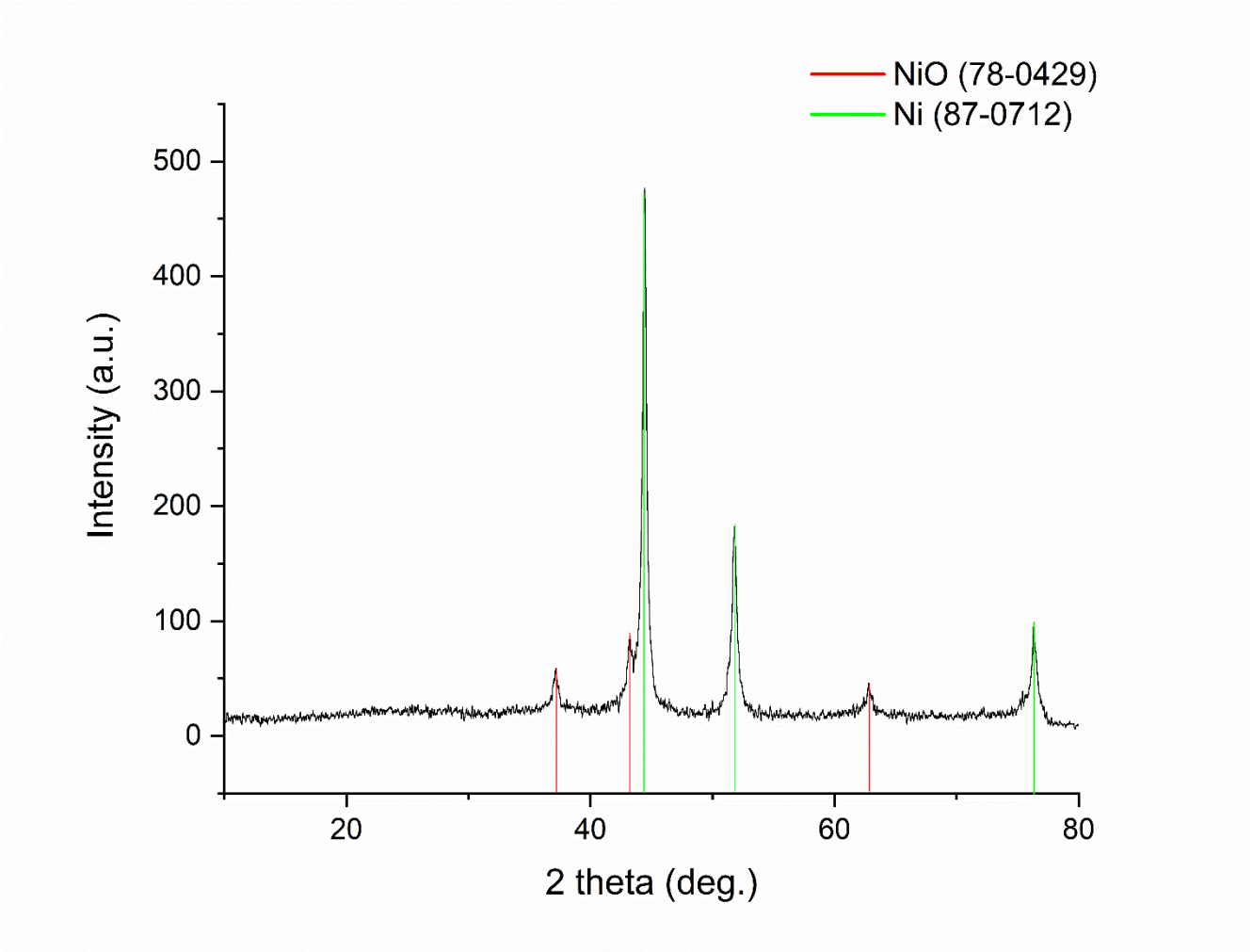

Figure S62. XRD of catalyst after reduction at 600 ℃.

Calculation of particles average size by Williamson-Hall method

With this linear equation we can find D:

$$\beta \cos\theta = 4\varepsilon \sin\theta + \frac{K\lambda}{D}$$

Where D = 52,6996 nm for 400 ℃.

D = 15,9165 nm for 600 ℃.